buildings

MDPI

Article

Evaluating the Effects of Climate Change on the Thermal Performance of Residential Buildings in Hot and Arid Regions

Khaoula Amraoui [1,*], Sara Ouanes [2], Safa Daich [1], Imadeddine Reghiss [3], Silvia Di Turi [4], Roberto Stasi [5] and Francesco Ruggiero [5]

[1] Department of Architecture, BERlab Laboratory, Mohamed Khider University of Biskra, Biskra 07000, Algeria; safa.daich@univ-biskra.dz
[2] Department of Architecture, LACOMOFA Laboratory, Mohamed Khider University of Biskra, Biskra 07000, Algeria; s.ouanes@univ-biskra.dz
[3] Department of Project Management, LAVMF Laboratory, University of Constantine 3, Constantine 25000, Algeria; imadeddine.reghiss@univ-constantine3.dz
[4] Energy Efficiency Unit Department (DUEE), Italian National Agency for New Technologies, Energy and Sustainable Economic Development (ENEA), 00123 Rome, Italy; silvia.dituri@enea.it
[5] Department of Architecture, Construction and Design (ArCod), Polytechnic University of Bari, 70125 Bari, Italy; roberto.stasi@poliba.it (R.S.); francesco.ruggiero@poliba.it (F.R.)
* Correspondence: khaoula.amraoui@univ-biskra.dz

Abstract

The main challenge for the scientific community is to mitigate climate change impacts while reducing energy consumption, without compromising comfort and quality of life. Buildings in hot climates require specific design strategies to limit the effects of extreme weather and heat waves. Standardized modern buildings, often unsuitable for hot and arid climates, lead to high energy consumption, mainly due to cooling systems, causing both discomfort and energy inefficiency. Previous studies have shown that solutions inspired by local vernacular architecture are often more effective than conventional construction techniques. This paper investigates the thermal response and discomfort intensity in two building models exposed to various climate scenarios: a typical modern residential building and a bioclimatic vernacular-inspired building. The analysis is conducted through dynamic thermal simulations under current as well as future medium- and long-term climate change scenarios. The study evaluates the buildings' ability to adapt to future environmental changes, an aspect that has not yet been studied in depth. Results show that contemporary buildings experience significantly higher levels of thermal discomfort than vernacular buildings under both present (TMY) and future (SSP1-2.6 and SSP5-8.5, 2080) climate conditions. Results show that under the present climate, the vernacular building exhibits about 22% fewer discomfort hours than the contemporary one and roughly half the overheating integrated degree-hours. Under future scenarios, overheating increases by 25.8% to 67.7% in the contemporary building and 36.1% to 89.6% in the vernacular building, yet the vernacular building consistently maintains substantially lower discomfort levels. Overall, vernacular inspired envelopes remain more resilient to warming in all scenarios, but additional adaptation measures are required to ensure acceptable summer comfort by late century.

Keywords: climate adaptability; thermal performance; climate change; SSP scenarios; thermal discomfort; residential buildings; hot and arid climate

Academic Editor: Apple L.S. Chan

Received: 30 September 2025
Revised: 24 November 2025
Accepted: 26 November 2025
Published: 2 December 2025

Citation: Amraoui, K.; Ouanes, S.; Daich, S.; Reghiss, I.; Di Turi, S.; Stasi, R.; Ruggiero, F. Evaluating the Effects of Climate Change on the Thermal Performance of Residential Buildings in Hot and Arid Regions. *Buildings* **2025**, *15*, 4378. https://doi.org/10.3390/buildings15234378

1. Introduction

In the context of climate change, the scientific community is paying increasing attention to its negative effects, which affect both the environment and human health, with the aim of preserving our planet, Earth's ecosystem, and ensuring the well-being of the occupants during the year [1]. Several studies reported that buildings consume more energy compared with other sectors, mainly for heating, cooling, and lighting with more than 36% of global energy consumption and emitted around 37% of CO_2 into the atmosphere [2,3]. This increased consumption of fossil fuels is expected to exacerbate global issues such as air pollution, respiratory and chronic diseases, and global warming [4,5].

In light of this issue, the energy efficiency of buildings has therefore become a global priority for sustainable development, particularly as energy consumption is constantly increasing. For this reason, it is imperative to identify solutions to reduce it and enhance the overall energy performance of the sector [6–9]. Indeed, the search for a zero-energy building with zero CO_2 emissions is becoming an important concern for several researchers [10,11].

In addition, the use of vernacular architecture, which involves designing buildings in harmony with local climatic conditions, available materials, and low-energy techniques, enhances occupant comfort while also reflecting regional cultural and socio-economic practices [12–15]. It relies on passive and bioclimatic strategies such as building orientation, daylighting, natural ventilation, and the thermal inertia of materials to optimize energy consumption while ensuring optimal comfort [16–19]. Previous studies indicate that the use of local materials reduces the carbon footprint and contributes to the economic autonomy of communities, while reflecting the history, culture and lifestyles of local citizens [20–23]. Numerous studies show that traditional architecture provides better interior comfort than modern buildings [24–30].

In addition, the use of vernacular architecture, which involves designing buildings in harmony with local climatic conditions, available materials, and low-energy techniques, enhances occupant comfort while also reflecting regional cultural and socio-economic practices [12,15,20,23]. In this context, several studies regarding the thermal performance of traditional buildings across different climatic conditions have shown that the integration of passive and bioclimatic strategies such as building orientation, daylighting, natural ventilation, and the thermal inertia of materials effectively contributes to reducing thermal discomfort by creating acceptable indoor thermal conditions for occupants and optimizing energy consumption [1,16,19]. The utilization of local materials is widely acknowledged to reduce carbon footprint and reinforce the economic autonomy of communities while reflecting historical, cultural, and lifestyle factors [20–23]. Extensive research demonstrates that traditional architectural approaches deliver better interior comfort than modern counterparts [24–30]. Vernacular architecture, which is tailored to local climatic conditions and applies low-energy design techniques, enhances comfort and represents regional socio-economic practices. Empirical studies have confirmed that integrating passive and bioclimatic strategies mitigates thermal discomfort and creates acceptable indoor thermal conditions while optimizing energy efficiency, with the building envelope recognized as a principal element for enhancing thermal performance [31–33]. The effectiveness of vernacular solutions is primarily due to their capacity to regulate indoor temperatures and respond to climatic constraints.

Case studies from Central Asia, Africa, and the Middle East highlight sustainable techniques such as massive walls, high ceilings, wind catchers, mashrabiyas, and courtyards with gardens and fountains as integral to improving indoor environmental quality in hot arid regions [31,32]. Questionnaire-based studies and field measurements indicate that Arabic vernacular architecture, and features like Mashrabiya, contribute to better thermal comfort and air circulation, although additional passive design strategies are sometimes

necessary for uniform performance throughout the day [33,34]. Numerical simulations and field surveys further illustrate that architectural elements like courtyards, green roofs, and passive cooling systems significantly lower energy demand compared to conventional designs, particularly for summer cooling loads [35]. Comparative analyses reveal that traditional dwellings consistently outperform contemporary ones thermally, irrespective of height or insulation placement. As global temperatures rise, traditional architecture continues to inspire adaptive, climate-responsive design, reducing reliance on mechanical systems and enhancing energy efficiency through features like caves, courtyards, high inertia envelopes, shading, and ground coupling [36]. Contemporary projects such as the Vilalta Mall in Addis Ababa integrate these traditional methods (façade perforations, open-air ventilation, solar panels, rainwater collection) while addressing local climate challenges, demonstrating the capacity of culturally inspired design to combine energy optimisation with occupant wellbeing [37].

Algeria's vernacular architectural heritage, particularly in the M'zab-Ghardaïa valley, Laghouat, El Oued, Ouled Djellal, Kabylie and the Aures, illustrates adaptation to local climatic conditions through specific forms, traditional materials and elements such as courtyards, domes, vaults and sunshades [38–45]. During the last decades, particularly after independence, Algeria has experienced considerable urban sprawl driven by population growth and increasing housing demand. This has led to the construction of standardized buildings often unsuited to local climatic conditions, forcing residents to resort to active cooling and heating systems in order to create a comfortable thermal environment, resulting in excessive energy consumption [46,47]. On the other hand, the lack of a link between contemporary design models, climatic conditions and specific socio-economic data has contributed significantly to the modification, and in some cases to the disappearance, of traditional models based on vernacular design. This situation leads to the emergence of a built environment that does not meet the requirements of comfort and is highly energy-intensive. Indeed, Alalouch et al. [48] reported that the abandonment of vernacular features in architectural design creates an imbalance between buildings and their surroundings, leading to discomfort and energy inefficiency.

Studies comparing traditional, modern, and contemporary architecture reveal that vernacular and traditional designs offer superior thermal comfort and lower energy consumption for cooling in hot climates. Djeddou et al. [49] found that traditional housing in Ouargla uses less cooling energy and provides better indoor comfort than modern and contemporary neighborhoods. Iftikhar et al. [50] showed similar results in Pakistan, with traditional homes staying cooler indoors compared to modern structures under identical conditions. Lotfabadi and Hançer [27] concluded that while increasing height in contemporary insulated buildings raises energy use without significantly improving comfort, vernacular architecture remains more effective. Amraoui et al. [51] demonstrated that passive cooling strategies from vernacular design can enhance comfort and reduce cooling demand by optimizing the building envelope, confirming the value of traditional solutions for climatic adaptability in hot, dry regions.

The literature review highlights that traditional architecture provides optimal year-round comfort while reducing buildings' overall energy demand. Furthermore, regions characterized by hot and arid climates, which are particularly vulnerable, are severely affected by the adverse impacts of climate change, especially during the summer hot days [52,53]. The use of these vernacular strategies could therefore be a sustainable solution in the face of the continuing rise in temperatures [54].

It is evident from the literature review that traditional architecture provides optimal year-round comfort while reducing the overall energy demand of buildings compared to modern and contemporary designs. Regions with hot and arid climates, which constitute

our case study are particularly vulnerable and are severely affected by the adverse impacts of climate change, especially during extremely hot summer days [32,46]. The use of vernacular strategies therefore represents a sustainable solution for cooling in the face of rising temperatures [47]. The most common and effective architectural strategies suitable for the regions under consideration can be broadly categorized according to their principal objectives. Strategies specifically aimed at cooling include the use of wind catchers or towers (malqaf) and techniques for evaporative cooling, both of which leverage local climatic resources to reduce indoor temperatures passively. In contrast, strategies focused on enhancing thermal comfort encompass mezzanines, vaults and domes, various solar shading devices, as well as decorative and functional elements such as mashrabiyyas and qamariyyahs, alongside green roofs.

On the other hand, the lack of a link between contemporary design models, climatic conditions and specific socio-economic data has contributed significantly to the modification, and in some cases to the disappearance, of traditional models based on vernacular design. This situation has led to the emergence of a built environment that does not meet comfort requirements and is highly energy-intensive, especially with the continuous increase in global temperatures. Indeed, Alalouch et al. [43] reported that the abandonment of vernacular features in architectural design creates an imbalance between buildings and their surroundings, leading to discomfort and energy inefficiency.

Moreover, under analogous climatic conditions, the majority of existing research has concentrated predominantly on evaluating thermal comfort and building efficiency in either historical or present contexts, often excluding future scenarios that may be significantly shaped by climate change. This paper, therefore, seeks to address this gap by firstly identifying and analyzing traditional design strategies that harness the natural environment for the development of efficient and sustainable buildings. Secondly, it aims to advance this comparatively under-investigated area through a comparative approach, assessing and contrasting the thermal response and intensity of discomfort in vernacular buildings versus contemporary constructions via dynamic simulations. Finally, the study endeavors to forecast the thermal performance of buildings under both current and future medium- and long-term climate change scenarios, with the ultimate goal of developing a predictive model that can facilitate adaptive responses to anticipated climatic variations.

2. Climate Models as Tools for Future Projections

Studies on the impact of climate change (CC) on the thermal and energy performance of buildings have grown considerably over the past two decades, reflecting an increasing interest in assessing future risks related to heating, cooling and indoor comfort. Numerous works have demonstrated that it is essential to integrate not only realistic climate data derived from global and regional climate models, but also advanced dynamic thermal simulation tools capable of reproducing building behavior under future climatic conditions. The approaches developed typically combine different time horizons, emission scenarios and building typologies, underlining both the methodological diversity and the importance of adapting energy planning strategies to local contexts.

Pioneering contributions, such as those by Asimakopoulos et al. [55], explored 13 Greek climate zones using TRNSYS to simulate three representative building types under various climate scenarios to anticipate heating and cooling needs. The authors of [56] further advanced this approach by assessing 153 residential buildings in Stockholm with Matlab/Simulink and several regional climate models, also incorporating projection uncertainties and passive cooling strategies. These studies converge on the idea that the reliability of simulations is directly linked to the robustness of the climate data employed.

The period between 2015 and 2017 witnessed a significant intensification of such studies. Shibuya and Croxford [57] evaluated changes in energy consumption in Japan and proposed CO_2 mitigation measures, while Hwang et al. [58] examined the impact of CC on a typical dwelling in Taiwan until the end of the 21st century using EnergyPlus. North American contributions broaden this field: Berardi and Jafarpur [58] developed a comparative methodology for various climate data generation tools applied to Toronto. In Sweden, Mata et al. [59] investigated the combined effect of CC and energy renovation measures over several decades, while Moazami et al. [60] examined in Geneva the sensitivity of energy performance results to the choice of weather datasets. These studies highlight the central role of climate database selection in predictive analysis.

In the European and Latin American context, Silvero et al. [61] assessed future thermal comfort in a heritage residential building in Asunción under RCP 4.5 and 8.5. In North America, Berardi and Jafarpur [62] compared RCM outputs with those generated by CCWorldWeatherGen and WeatherShift for 16 buildings in Toronto. At the same time, Haddad et al. [63] applied this approach in Darwin (Australia), studying air-conditioning systems and adaptation strategies. Similar directions are found in Scandinavia, where Perera et al. [64] projected the future energy demand of 153 buildings in Stockholm under several scenarios (RCP 2.6, 4.5 and 8.5) using Matlab/Simulink. Stagrum et al. [65] review climate change adaptation for buildings, emphasizing challenges from rising temperatures and the need for integrating future climate scenarios for resilience, especially in warmer climates, and the call for more empirical research in colder regions. Nguyen et al. [66] assess climate change impacts on energy and thermal performance of Southeast Asian office buildings using multi-objective optimization with a calibrated Hanoi baseline and 200 probabilistic variants. Simulations under RCP4.5 and RCP8.5 scenarios show a 7.2–12.3% rise in annual energy use and extended overheating, especially in Bangkok and Kuala Lumpur. Optimized designs reduce solar gains, internal loads, leaks, and use night ventilation but cannot fully maintain current comfort levels. Calama-González et al. [67] investigate the thermal comfort of type H social housing in southern Spain through a case study of a 4-story building in Cordoba, using calibrated energy simulations combined with statistical methods, identifying winter undercooling as the main issue with an average of 68 discomfort hours annually. In London, Salvati and Kolokotroni [68] adapted weather file generation to urban specificities to simulate the evolution of a terraced house.

The study by Tootkaboni et al. [69] in Rome tested three climate tools (WeatherShift, CCWorldWeatherGen, Meteonorm), illustrating the growing diversification of methodologies to generate TMYs adapted to future projections. More recently, Hosseini et al. [70] and Kazanci et al. [71] examined in Sweden and Denmark the energy requirements of residential and office buildings, respectively, incorporating the urban heat island dimension and comparing cooling systems. Rahif et al. [72] projected the risk of overheating in NZEB dwellings in Brussels. Machard et al. [73] refined the sensitivity analysis of collective housing, examining the relationships between design parameters and overheating risks. Rodrigues et al. [74] introduce an open-source Future Weather Generator tool that produces future hourly weather data for building energy simulations using latest climate models, demonstrated in a Portuguese office building with shifts in heating and cooling demands, enhancing climate impact analysis capabilities with high resolution and customization. In China, Qian et al. [75] focused on Harbin, Beijing and Chengdu, comparing different TMY construction methods and their influence on indoor overheating. Park et al. [76] explored in South Korea the performance of innovative façade systems for high-rise residential towers, simulating throughout the 21st century under RCP 8.5.

Wehbi and Messadi [77] focus on the development of a multi-storey, multi-generational low-carbon Passive House in Fayetteville, Arkansas, USA, examining challenges in the

preconstruction phase including management, sustainable design integration, regulatory compliance, professional expertise, material sourcing, and software tool usage. Hostein et al. [78] present a methodology using a calibrated thermo-aeraulic model to simulate indoor overheating in an energy-efficient renovated apartment in Lyon, France, showing drastic increases in thermal discomfort under future climate scenarios, particularly under the high-emission RCP 8.5, where ventilation strategies and occupant behaviors significantly influence outcomes, highlighting the need for passive cooling and occupant education in building renovations to mitigate future urban overheating risks. In 2025, Mulverhill et al. [79] project significant increases in wildfire burn probability across Canada's forested Eco-zones and communities throughout the 21st century under various future climate scenarios, emphasizing the need for improved wildfire management and adaptive planning despite limitations in static vegetation assumptions. Duan et al. [2] review 212 studies on simulating climate change effects on building thermal performance, highlighting a feedback loop of warming, increased cooling demands, and emissions. They identify data quality issues, geographic research gaps, and methodological inconsistencies, emphasizing the need for standardized approaches, urban heat island and extreme weather integration, updated SSP scenarios, occupant behavior modeling, and interdisciplinary collaboration for resilient, efficient building design.

To anticipate the evolution of global climate, researchers rely on climate change scenarios generated through numerical climate models. These models are essentially large computer codes that reproduce, in a simplified form, the physical and chemical processes governing the atmosphere, oceans, land surface, cryosphere, and biosphere [80]. Each of these models simplify, in a unique way, the real processes in the climate balancing complexity with computational feasibility. As the representation of these processes varies, multiple General Circulation Models (GCMs) were developed across the globe. Their diversity allows exploring uncertainties across different representations of the Earth system.

The Coupled Model Intercomparison Project (CMIP) has coordinated experiments among climate research centers worldwide. Its objective is to harmonize experiments, benchmark models against common protocols, and provide datasets for assessment [81]. Its most recent phase, CMIP6, provided the data for the IPCC Sixth Assessment Report [82]. The Intergovernmental Panel on Climate Change (IPCC) summarizes the results of many ensembles of CMIP models, highlighting both agreements and uncertainties [83].

2.1. Evolution of Climate Change Scenario Frameworks

The description of future climates has evolved through successive scenario frameworks as shown in Table 1. Early assessments figured in the third Assessment Report of the IPCC (AR3) and relied on the Special Report on Emissions Scenarios (SRESs). SRESs described alternative futures based on demographic, economic, and technological pathways, without explicit climate policy assumptions [84]. Years later, the framework shifted to Representative Concentration Pathways (RCPs) in AR5. This time, RCPs defined trajectories of radiative forcing (measured in W/m^2 by 2100), ranging from strong mitigation (RCP2.6) to high-emission futures (RCP8.5) [85]. Most recently, in AR6, the IPCC adopted the Shared Socioeconomic Pathways (SSPs), which combine socioeconomic narratives with corresponding climate forcing levels (SSP1-2.6 to SSP5-8.5) [86,87]. SSPs allow researchers to link human development pathways with greenhouse gas trajectories more explicitly than previous frameworks.

Table 1. Overview of climate scenario frameworks used in IPCC reports.

Framework	Description	IPCC Assessment Report		CMIP Phase	Climate Change Scenarios and Main Feature	
Special Report on Emissions Scenarios (SRESs)	Describes alternative futures based on population, economy and technology	AR3	2001	CMIP3	A1	Rapid economic growth
					A2	High population growth
		AR4	2007		B1	Global sustainability
					B2	Local sustainability
Representative Concentration Pathways (RCPs)	Focuses on radiative forcing levels by 2100 (W/m^2)	AR5	2014	CMIP5	RCP2.6	Strong mitigation
					RCP4.5	Intermediate stabilization
					RCP8.5	High emissions
Shared Socioeconomics Pathways (SSPs)	Links socioeconomic development pathways with radiative forcing levels	AR6	2021	CMIP6	SSP1-2.6	sustainability
					SSP2-4.5	Middle off road
					SSP3-7.0	Regional rivalry
					SSP4	Mixed world
					SSP5-8.5	Fossil fuel growth

2.2. Future Weather Generator: A Morphing Tool Integrating CIMP6

Several morphing tools have been developed to transform weather files into future weather datasets. Among the most cited are WeatherShift, Weather Morph, and CC-WorldWeatherGen, each with limitations such as coarse resolution, reliance on older IPCC scenarios, and dated baseline periods [74]. More recently, the Future Weather Generator [74] has been introduced as an open-source alternative that incorporates the latest CMIP6 data. The Future Weather Generator tool was developed in collaboration between academic and research institutions as a free, open-source Java application. It morphs present-day hourly weather data in .epw format into future weather files by applying climate change signals from CMIP6 and climate models.

The tool accounts for greenhouse gas scenarios by implementing the most recent scenarios of climate change, namely, SSP1-2.6, SSP2-4.5, SSP3-7.0, and SSP5-8.5 pathways, and generates projections for mid-term (2050: 2036–2065) and late-term (2080: 2066–2095) frameworks. Future weather files are created by adjusting monthly average and variability values. A wide set of GCMs is available, offering flexibility in exploring both single and an ensemble of climate futures. In this study, the tool was used to generate epw files for simulations, ensuring consistency with IPCC scenarios and supporting the assessment of building performance under different climate change pathways. It was chosen to rely on ensemble of multiple GCMs rather than relying on a single projection which aligns with recent research.

3. Methodology

A methodological approach combining literature review, an examination of local construction practices and thermal modelling was adopted, as illustrated in Figure 1. First, an in-depth study of the literature identified the key parameters related to vernacular architecture and thermal performance in hot, dry climates, as well as analyzing current construction practices through a quantitative assessment of selected buildings. Next, a thermal model of each building was developed using DesignBuilder/EnergyPlus software, calibrated and validated using technical data and on-site measurements.

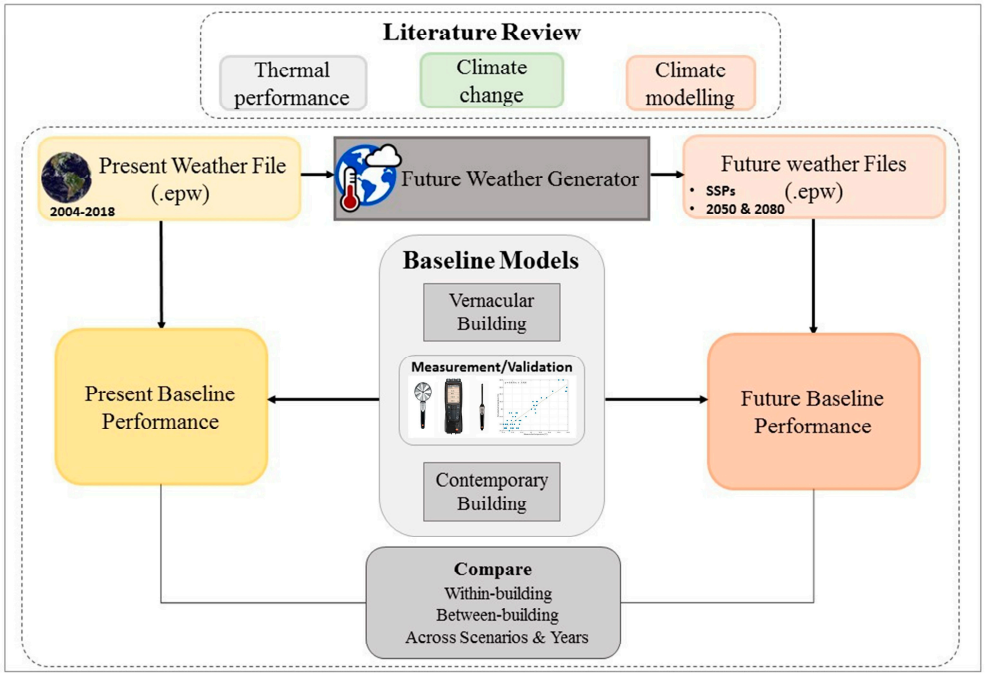

Figure 1. Study conceptual framework (Source Authors, 2025).

The next step began with the creation of hourly future climate weather data files, generated from a recent .epw file for the period 2004–2018. To capture a range of possible future climate conditions, four distinct socioeconomic scenario pathways were selected: SSP1 (a pathway focused on sustainability and equity), SSP5 (rapid development driven by fossil fuels), SSP3 (a fragmented world with regional rivalry), and SSP2 (an intermediate scenario reflecting mixed policy approaches). Combined with two target years (2050, 2080), this led to the production of eight future weather files, complementing the original typical meteorological year (TMY) file.

For the simulation phase, each of these weather files was individually used to run building performance scenarios. For each scenario, data was collected at monthly, daily, and hourly time steps to ensure a robust and detailed analysis of climate impacts on building performance. The resulting outputs from mid-term and late-term projections under each scenario were critically compared with the baseline results derived from the TMY file. This comparative analysis allowed assessment of the potential impacts of different climate futures on building energy performance and thermal comfort.

After conducting a thermal analysis of the two buildings, a verification of thermal comfort will be carried out using two indicators: the adaptive model of the ASHRAE 55-2023 [88] standard and the integrated discomfort index. This evaluation will cover both the current summer period derived from the typical meteorological year (TMY) file and the worst scenario projected for the year 2080. Thermal comfort was evaluated using the adaptive model of ASHRAE 55-2023 for naturally ventilated buildings. In this approach, the acceptable indoor operative temperature is expressed as a function of the prevailing outdoor temperature Tpma(out). The 80% and 90% acceptability limits are defined by the following equations:

$$Upper\ 80\%\ acceptability\ limit = 0.31T_{pma_{(out)}} + 21.3\ [^{\circ}\mathrm{C}] \quad (1)$$

$$Lower\ 80\%\ acceptability\ limit = 0.31T_{pma_{(out)}} + 14.3\ [^{\circ}\mathrm{C}] \quad (2)$$

$$Upper\ 90\%\ acceptability\ limit = 0.31T_{pma_{(out)}} + 20.3\ [^{\circ}\mathrm{C}] \quad (3)$$

$$Lower\ 90\%\ acceptability\ limit = 0.31T_{pma_{(out)}} + 15.3\ [^{\circ}C] \quad (4)$$

Following Zhang et al. [89], in free-running conditions the indoor air temperature is approximately proportional to the space cooling (or heating) load. When internal heat gains and air-change rates do not vary significantly, the thermo-physical properties of the building envelope largely govern the thermal response of the space. Under this assumption, the comparison between the two case studies can be interpreted primarily as a comparison of the building envelope performance, rather than of differences in operation or internal loading. This can be presented by the integrated thermal discomfort degree index in the following equation:

$$\mathrm{I_{sum}} = \int_{summer} (T_{in} - T_h)dt\ when\ T_{in} > T_h [^{\circ}\mathrm{C{\cdot}h}] \quad (5)$$

where T_{in} is the indoor operating temperature, T_h is the thermal comfort temperature reference, and dt is the time step of the simulation, in our case 1 h.

The comparative analysis between the two case studies is intentionally focused on indoor thermal response and comfort-related indicators, namely operative temperature (adaptive model) and integrated summer discomfort degree. These indicators do not scale with total floor area or volume and therefore allow a direct comparison of passive behavior under equivalent boundary conditions. In both models, simulations were run in free-running mode, with no active cooling or heating, no internal gains, and similar exposure (orientation), in order to isolate envelope-driven effects rather than operational control.

4. Context and Climate

Biskra and Ouled Djellal, two cities in southeastern Algeria, were once a single city, Biskra (Figure 2a), before an administrative decision in 2021 divided them into two distinct communes (Figure 2b). Situated at the southern foothills of the Saharan Atlas Mountains, these two cities share the same climatic conditions characterized by a hot desert climate typical of the Saharan region, with long and extremely hot summers and mild winters. Precipitation is very limited, mainly concentrated in autumn and winter, while summers are very dry. The average annual temperature is around 22–23 °C, with summer maximums frequently exceeding 40 °C, and extreme peaks surpassing 50 °C.

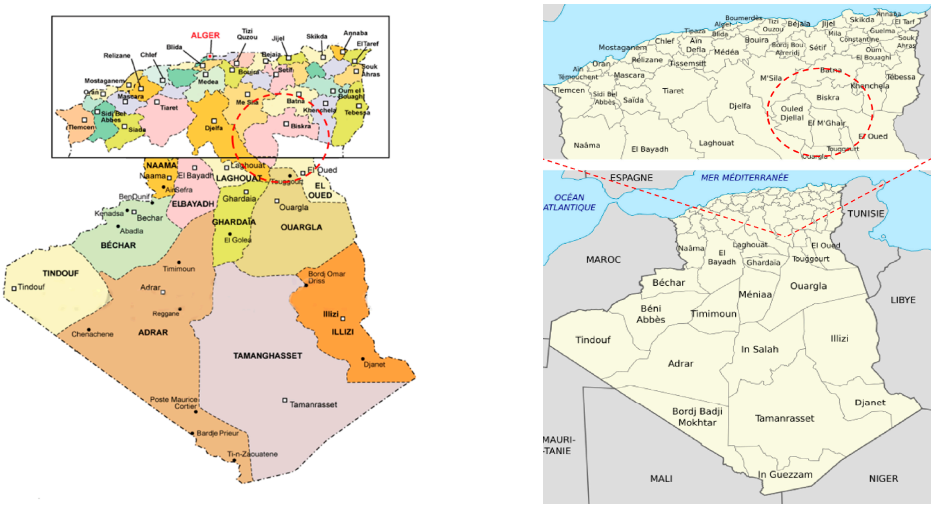

(**a**) (**b**)

Figure 2. Geographic Location of Biskra and Ouled Djellal within the Algerian Context: (**a**) Unified Urban Area: as a Single City; (**b**) Administrative Division: as Distinct Towns.

The graph below in Figure 3 represents the monthly variation of mean air temperature (Ta) in degrees Celsius and relative humidity (RH) in percentage for the city of Biskra, which is situated in a hot arid climate zone and serves as the study context. The graph shows that Biskra experiences marked seasonal fluctuations, with mean temperatures steadily increasing from approximately 10 °C in January to peaks above 32 °C during July and August, before declining towards 13 °C in December; concurrently, relative humidity presents an inverse pattern, starting around 55% during the winter months, reaching minimum values close to 25–26% in the hot summer.

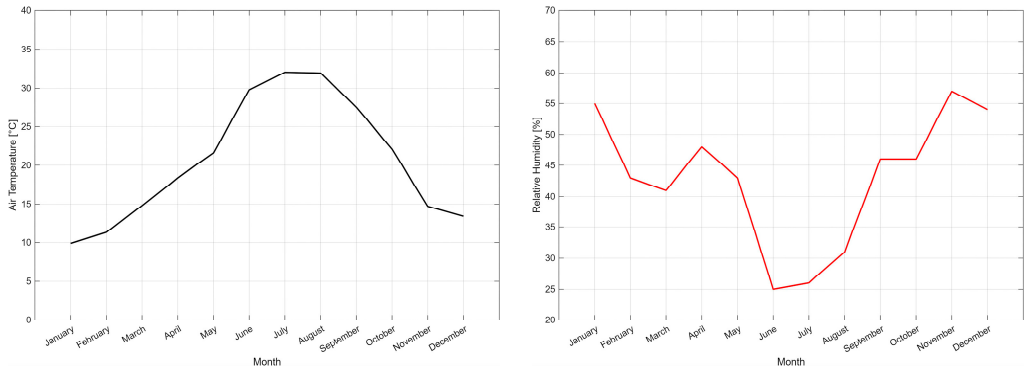

(**a**) (**b**)

Figure 3. Climate weather data: (**a**) Monthly temperature; (**b**) Monthly humidity (Source Meteonorm, processed by Authors, 2025).

5. Case Study

5.1. Presentation of Case Studies

To assess the behavior of buildings in different future climate scenarios, two types of residential buildings were selected, differing mainly in the nature and treatment of their envelope.

The contemporary building (first case study), shown in Figure 4a, is an apartment located in 44 housing units, Al Alia, Biskra. It was selected as a representative example of Algerian public housing in terms of typology, scale, and construction materials. The building envelope is composed of double-walled exterior walls made of hollow bricks, with the exterior surface finished in cement plaster and the interior surface finished in plaster. The ceilings of the dwellings consist of multiple layers, including a plaster coating, a hollow core incorporating a compression slab, a mortar layer, and a floor covering, as illustrated in Figure 4b.

The vernacular building (second case study), illustrated in Figure 5a, forms part of the 200 housing units in Ouled Djellal and is constructed entirely from local materials. The external walls are composed of locally quarried gypsum stone and finished with a plaster coating to enhance thermal performance and regulate humidity (Figure 5b).

The roofs are constructed using concrete frameworks filled with lime sandstone and covered with reinforced concrete. The roof comprises several layers as shown in Figure 4b: a granite tile finish, a cement layer, a hollow concrete block slab, and an internal plaster layer. The choice of lime sandstone was a practical one, well suited to the regional climate and reflecting local architectural traditions. Cement was used in the construction of beams and roofs, and when mixed with pulverized lime and sand, served as mortar [90]. The thermophysical characteristics of the materials used in both case studies are summarized in Table 2.

(**a**) (**b**)

Figure 4. (**a**) Outdoor façade of the first case study; (**b**) external walls and roof Components (Source: Authors, 2025).

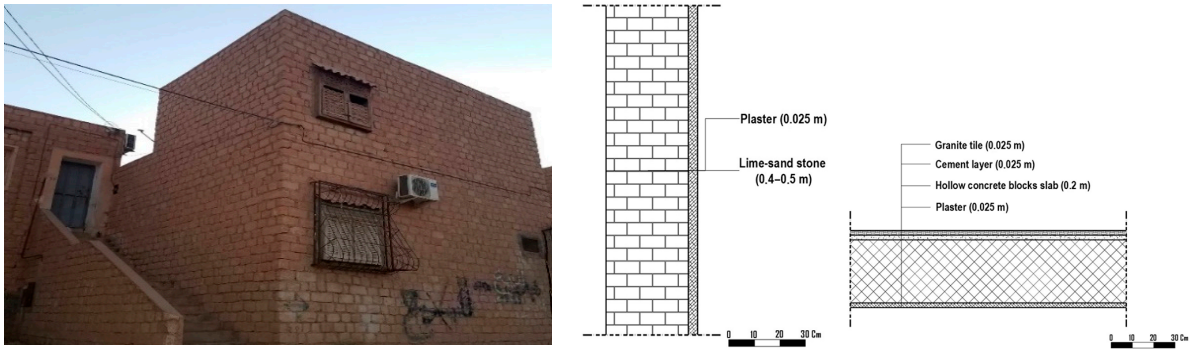

(**a**) (**b**)

Figure 5. (**a**) Outdoor façade of the second case study; (**b**) external walls and roof component (Source: Authors, 2025).

Table 2. Materials thermophysical properties [91].

	Material	Density (kg/m^3)	Thermal Capacity (J/kg·K)	Conductivity (W/m·K)	Thickness (m)	Heat Transfer Coefficient (W/m^2·K)
Contemporary building (First case study)	Wall composition					
	Cement plaster	2200	1080	1.4	0.015	1.321
	Hollow brick	900	936	0.48	0.15	
	Air gap			0.31	0.05	
	Hollow brick	900	936	0.48	0.1	
	Gypsum plaster	875	936	0.35	0.015	
	Roof composition					
	Gypsum plaster	875	936	0.35	0.015	2.55
	Hollow concrete reinforced slab	1450	1080	1.45	0.2	
	Mortar	2200	1080	1.4	0.04	
	Floor covering	1900	936	2.1	0.06	
	Single clear glazing				0.004	5.871
Vernacular building (Second case study)	Wall composition					
	Lime-sand stone	1982	1910	0.93	0.4	1.489
	Plaster	875	936	0.35	0.025	
	Roof composition					
	Granite tile	2200	936	2.1	0.025	1.964
	Cement layer	2200	1080	1.4	0.025	
	Hollow concrete blocks slab	1450	1080	1.45	0.2	
	Plaster	875	936	0.35	0.025	
	Single clear glazing				0.004	5.871

5.2. Simulation Model Setup

Thermal simulations make it possible to get as close as possible to real conditions and to test several parameters at the same time.

Using DesignBuilder V7/EnergyPlus 9.4, the first step in the simulation process is to insert the climate file for the study region. Next comes the building modelling stage, which involves creating the virtual model and its geometric description. During the modelling phase, choices must be made regarding shapes, materials (opaque and glazing), etc. These elements are placed in the software library. The user can then associate the different elements of the following objects (building zones, workplace, etc.). After creating the models and in order to validate them, the simulations were performed in neutral conditions, where all equipment was deactivated (air-conditioning, heating, artificial lighting and mechanical ventilation), while internal gains due to occupancy were considered zero.

A comprehensive three-dimensional (3D) model of the building and its internal spatial configuration was developed using DesignBuilder V7. This model accurately represents the architectural form, material compositions, and construction assemblies, thereby faithfully reflecting the building envelope, windows, shading elements, and internal zoning of the case study (Figures 6 and 7). The building envelope components, including walls, roofs, floors, windows, and doors, were modelled as multi-layered assemblies composed of materials characterized by their essential thermal properties: thickness, thermal conductivity, density, and specific heat capacity. These properties fundamentally govern heat transfer mechanisms such as conduction, thermal storage (thermal mass), and radiation.

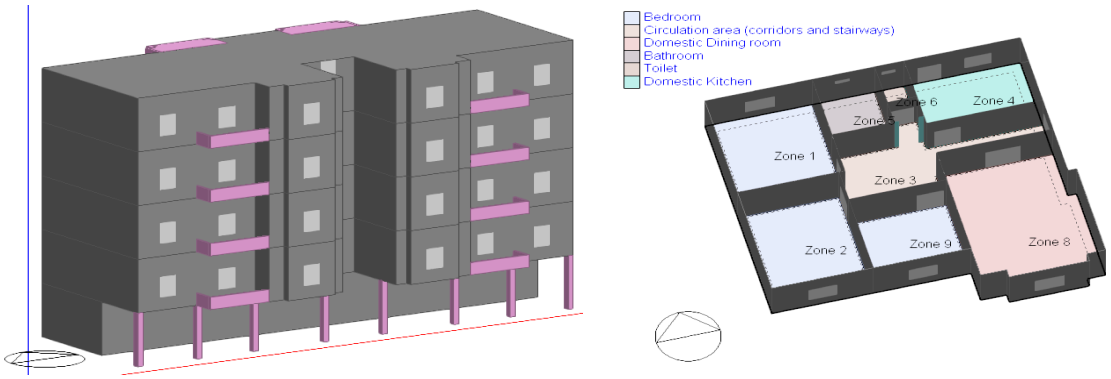

(**a**) (**b**)

Figure 6. (**a**) DesignBuilder model of the first case study; (**b**) Case study spatial zoning.

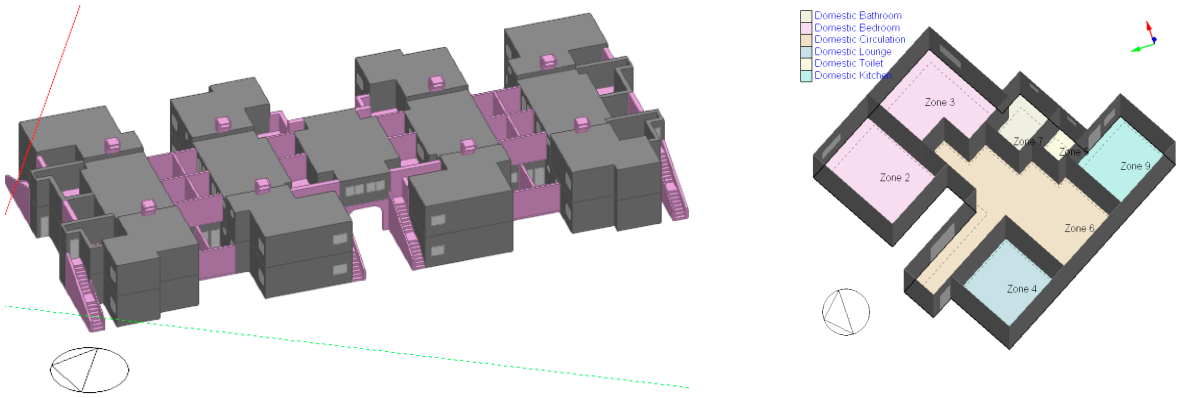

(**a**) (**b**)

Figure 7. (**a**) DesignBuilder model of the second case study; (**b**) Case study spatial zoning.

To ensure that the simulation outputs replicate actual operational conditions, real hourly weather data corresponding to the building's geographic location was applied. This dataset, sourced from Meteonorm [92], ensured the incorporation of capturing authentic climatic variations throughout the simulated period. Infiltration rate was calculated in accordance with the Regulatory Technical Document (DTR C3-2) equation (Equation (5)), ensuring the model's fidelity to real airflow phenomena affecting indoor thermal conditions. These rigorous modelling practices, combined with detailed construction specifications and site-specific boundary conditions, align with methodologies widely adopted and validated in peer-reviewed literature and standards such as those of ASHRAE 55-2023.

The use of a simulation model requires the application of indicators to assess its reliability in relation to measured data. In accordance with ASHRAE Guideline 14–2014 [93], validation is based on two main statistical indicators: the mean bias error (MBE) (Equation (6)), whose value must be between −10% and +10%, and the coefficient of variation of the root mean square error CV(RMSE) (Equation (7)), which must remain below 30%. These criteria ensure a satisfactory correspondence between the simulated model and reality. Furthermore, to reinforce the robustness of the validation, it is essential to consider all sources of uncertainty, both internal (related to the model and its parameters) and external (related to environmental conditions (Equation (8)), and the quality of experimental measurements [41–44].

$$\boldsymbol{MBE} = \frac{\sum_{i=1}^{n}(\boldsymbol{y_i} - \boldsymbol{x_i})}{\boldsymbol{n}} \cdot 100\ [\%] \tag{6}$$

$$\boldsymbol{cvRMSE} = \frac{1}{\overline{\boldsymbol{y}}}\left(\frac{\sum_{i=1}^{n}(\boldsymbol{y_i} - \boldsymbol{x_i})^2}{\boldsymbol{n}}\right)^{1/2} \cdot 100\ [\%] \tag{7}$$

where

y_i is the measured value; x_i is the simulated value;
n is the number of measures; $\overline{y}$ is the mean value of measured data.

The coefficient of determination, R^2, is another commonly used indicator. It is calculated using Equation (4) and indicates how closely the simulated values align with the regression line of the measured data. Ranging between 0 and 1, it is recommended to obtain a value of at least 0.75 for a properly calibrated model [94,95].

$$R^2 = \left(\frac{n \cdot \sum_{i=1}^{n} y_i \cdot x_i - \sum_{i=1}^{n} y_i \cdot \sum_{i=1}^{n} x_i}{\sqrt{\left(n \cdot \sum_{i=1}^{n} y_i^2 - \left(\sum_{i=1}^{n} y_i\right)^2\right) \cdot \left(n \cdot \sum_{i=1}^{n} x_i^2 - \left(\sum_{i=1}^{n} y_i\right)^2\right)}}\right)^2 \tag{8}$$

The comparison between indoor air temperatures measured in situ and those simulated allows assessing the accuracy of the thermal model. The second case study has already been evaluated and calibrated by the authors in a previous study [29]. For the first case study, instead, experimental measurements were carried out in two rooms of the dwelling (Figure 8), namely the living room (Zone 8) and the hall (Zone 3), under natural conditions and using a Testo 480 instrument (accuracy: ±0.3 °C + 0.1% of measured value). The recordings were made over a period of four days, at two-hour intervals.

In order to ensure optimal representativeness of actual conditions and to provide an accurate assessment of the thermal comfort generated by the two envelope systems studied, the measurements were conducted under similar conditions for both buildings. They were therefore taken into rooms facing south-west, at the center of the room, at a height corresponding to that of a seated person, approximately 1.10 m above the floor. Furthermore, temperature readings were taken under natural conditions, i.e., without the use of mechanical air conditioning, with windows and blinds open in accordance with

normal occupancy patterns. Several parameters were considered in order to limit bias, i.e., the space was unoccupied, and all electrical appliances had been switched off beforehand, with the aim of minimizing the influence of internal gains on the measurements.

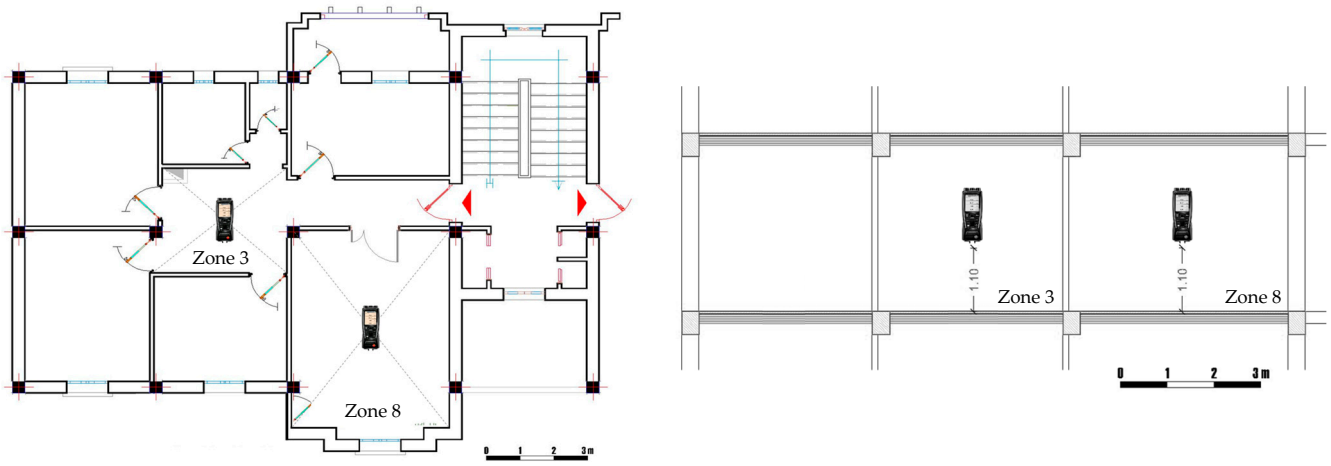

(**a**) (**b**)

Figure 8. Illustration of the instrument positioning (**a**) at the plan level; (**b**) at the sectional level.

The graphs in Figure 9a illustrate that the recorded and simulated temperatures in the living room (Zone 8) generally remain within a narrow range of approximately 32 to 34 °C. More specifically, it can be observed that in the morning and early afternoon, temperatures fluctuate around 32.5 °C, indicating relative stability. From late morning onwards, there is a slight increase in temperatures, peaking at midday. This rise is followed by a series of more pronounced variations in the afternoon and evening, reflecting the thermal dynamics linked to environmental conditions and the use of spaces. Overall, Figure 9b reveals a strong linear correlation between the two datasets and supporting the reliability of the simulation results.

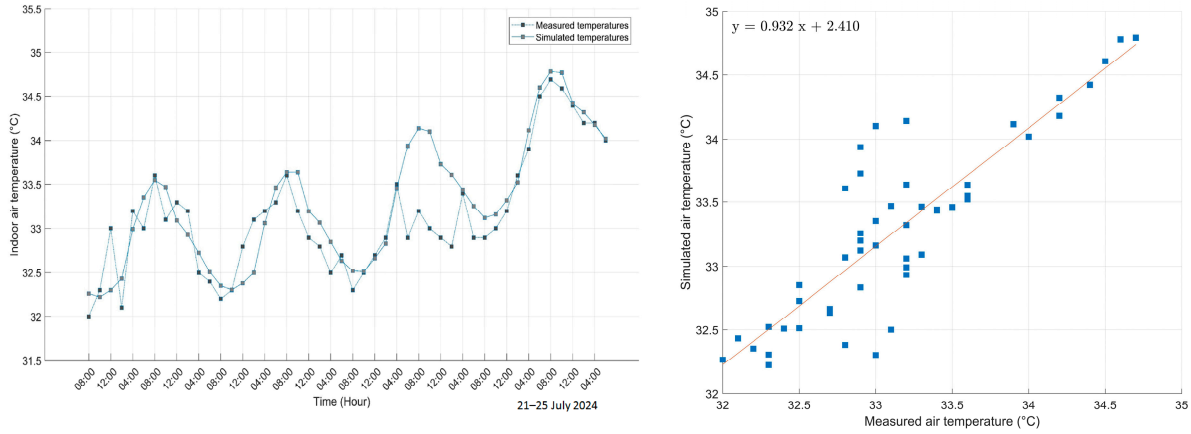

(**a**) (**b**)

Figure 9. First case simulated and measured indoor air temperature in Zone 8 (**a**) temporal variations; (**b**) correlation.

Figure 10a shows a comparison between the measured and simulated indoor air temperatures in the hall (Zone 3), demonstrating a strong coherence as both recorded and modeled values remain within a narrow range of 31 to 33.5 °C, with both sets of data following similar trends and remaining within a narrow temperature range of approximately 31 to 33.5 °C. The simulated temperatures generally reflect the daily variations

observed in the measured data, including morning stability around 31.5 °C and a gradual rise towards mid-afternoon peaks close to 33 °C. Slight discrepancies appear at certain times when measured temperatures show more pronounced fluctuations, probably due to local environmental factors or transient conditions that are not fully accounted for in the model. Overall, the strong agreement between measured and simulated temperatures, as shown in Figure 10b demonstrates the robustness and accuracy of the simulation model in representing the thermal behavior of the indoor environment.

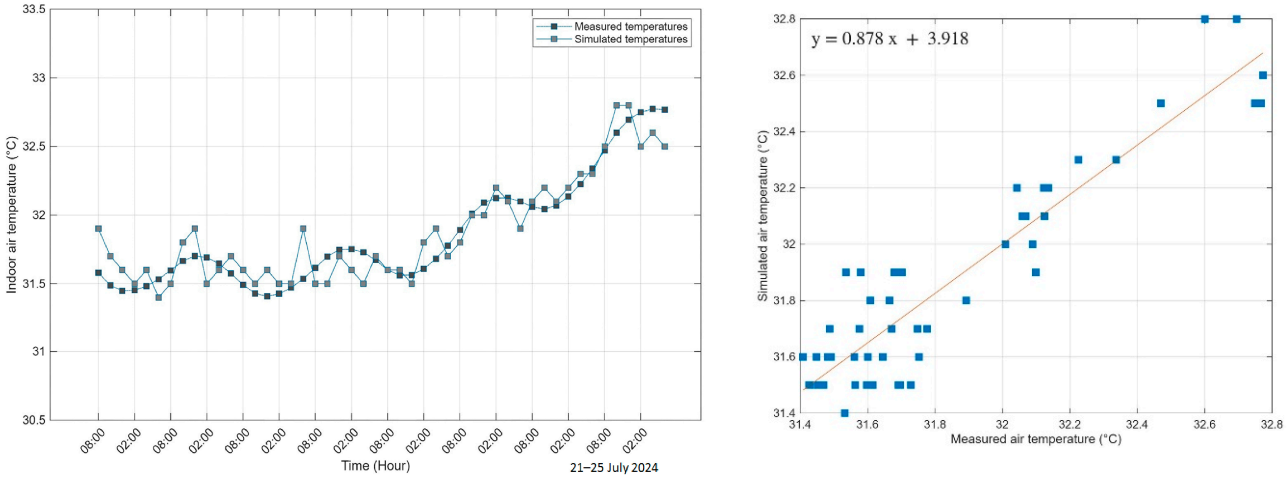

(**a**) (**b**)

Figure 10. Second case simulated and measured indoor air temperature in Zone 3 (**a**) temporal variations; (**b**) correlation.

The measured and simulated values frequently intersect throughout the entire period, indicating that the model accurately predicts indoor temperature variations. This strong agreement between experimental and simulated data validates the model and demonstrates that the model reliably replicates the actual thermal behavior of the analysed building. The validation metrics, presented in Table 3, support this conclusion, with Mean Bias Error (MBE) values of −0.18% for Zone 3 and 0.06% for Zone 8, coefficient of variation of the root mean square error (cvRMSE) values of 0.72% for Zone 3 and 0.47% for Zone 8, and determination coefficients (R^2) of 0.89 for Zone 3 and 0.86 for Zone 8. These results confirm the model's reliability and relevance for future predictive simulations of indoor temperature dynamics.

Table 3. Validation Indices for Indoor Temperature Simulation in Selected Zones.

Validation Indices	Living Room (Zone 8)	Hall (Zone 3)
MBE [%]	−0.18	0.06
cvRMSE [%]	0.72	0.47
R^2	0.89	0.86

6. Results and Discussion

6.1. Current and Projected Evolution of Temperature Under SSP Scenarios for Mid and Long Terms

Figure 11 illustrates the monthly mean dry-bulb temperature for the present climate and for future scenarios generated using the Future Weather Generator under different Shared Socioeconomic Pathways (SSPs) for mid-term (2050) and late-term (2080). Overall, the curves show a consistent warming trend across all SSP scenarios compared to the

present climate, with the magnitude of warming depending on both the emission pathway and the time horizon.

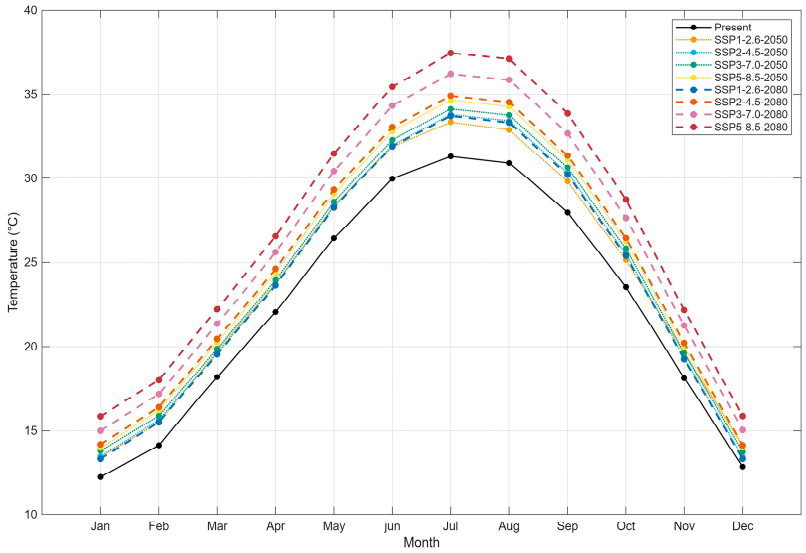

Figure 11. Present and future weather.

The shape of the curves remains similar across all scenarios, with the highest temperatures in July and August and the lowest in January and February, reflecting the preserved seasonal cycle. For the mid-term framework, projected temperatures rise by approximately 2–4 °C relative to present, with lower warming under SSP1-2.6 and higher under SSP5-8.5. For late-term framework, the warming intensifies, with increases reaching 5–7 °C under SSP5-8.5. Even the low-emission pathway (SSP1-2.6) shows noticeable warming compared to present.

The difference between pathways is already visible by 2050, but it becomes more pronounced by 2080, especially during the summer period. For example, the July monthly mean temperature under SSP1-2.6 is lower than under SSP5-8.5 by roughly 0.9 °C in mid-century and about 3.9 °C by late century. In practice, the choice of pathway therefore corresponds to several degrees of mean monthly temperature during the peak cooling season. This means that adaptation measures sized according to one pathway may be under- or over-designed if the actual climate trajectory follows a different SSP. Evaluating building response under all scenarios, rather than only a single "worst case," aligns the study with current practice in climate impact research.

The shape of the seasonal cycle is preserved across scenarios, suggesting that the dominant effect is an upward shift in temperature rather than a phase change in seasons, primarily due to the mathematical models predicting climate change. However, peak summer months warm more than transition months such as April and October. For building performance, this implies a disproportionate rise in cooling loads, overheating risk, and outdoor thermal stress under high-emission pathways, especially toward the end of the century, while winter heating demand becomes relatively less critical.

The different scenarios do not only show similar qualitative trends; they also diverge in both magnitude and seasonal emphasis. In all cases, the projected temperature increase is non-negligible, even for mid-century pathways, and must be accounted for in the design and retrofitting of buildings in hot–arid regions. In short, the graph shows that Biskra will experience significant warming under all scenarios, with the most severe increases projected for high-emission futures (SSP3-7.0 and SSP5-8.5), particularly by 2080.

6.2. Thermal Response of the Two Case Studies in the Current Climate Conditions (TMY Scenario)

Figure 12 compares the monthly temperatures simulated inside the two validated buildings models with the outdoor temperature throughout the year (TMY climate conditions). The results for the first case study (contemporary building) show indoor temperatures close to the outdoor temperature, with significant seasonal variations: in summer, indoor temperatures sometimes exceed 35 °C, while in winter, they drop to around 15 °C, following the rise and fall of the outdoor temperature, which varies from 10 °C to nearly 45 °C.

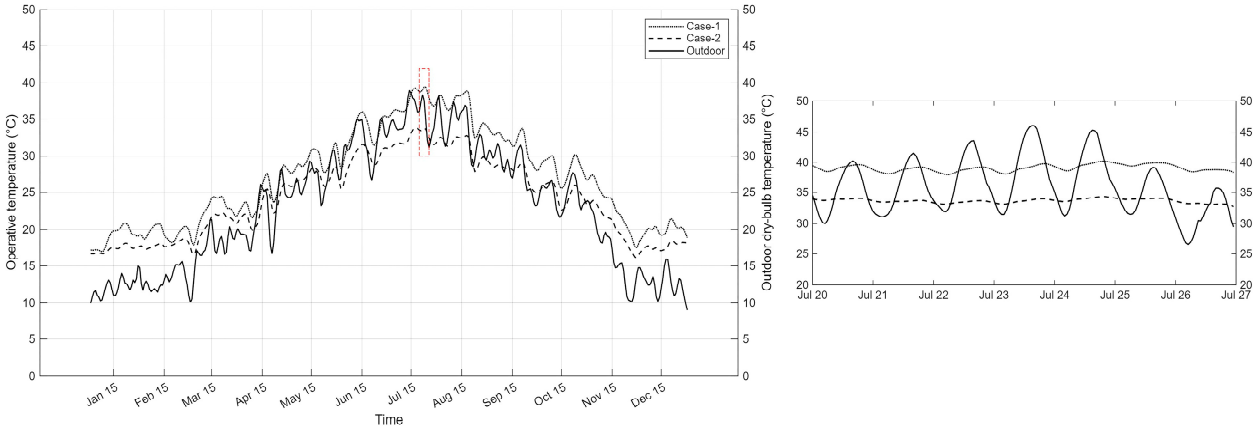

Figure 12. On the left, comparison between actual monthly temperature variations (TMY); on the right, close examination of the hottest week from the red box on the left.

For the second case study (building inspired by vernacular architecture), indoor temperatures are more stable and less extreme: summer peaks are reduced, temperatures often remain below 35 °C, and winter lows are softened, rarely falling below 20 °C. This curve is therefore less close to the extremes observed outside. The comparison highlights a stronger influence of the outdoor environment on the contemporary building, while the bioclimatic building benefits from better thermal insulation and passive regulation, allowing for superior thermal comfort and a reduction in indoor temperature fluctuations throughout the year.

The graph shows that the building inspired by vernacular architecture ensures a more stable and comfortable indoor temperature throughout the year, with significant attenuation of summer and winter thermal extremes, compared to the contemporary building whose indoor temperatures follow the outdoor temperature more closely and variably, thus exposing occupants to greater fluctuations.

In addition to the seasonal trends, the graphs also reveal pronounced diurnal (day-to-night) temperature fluctuations for both outdoor and indoor environments. The outdoor temperatures display a clear daily cycle with sharp increases during the day and marked decreases at night, especially evident during the summer period, where differences can exceed 20 °C within a single day. The contemporary building's indoor environment largely mirrors these rapid shifts, exposing occupants to uncomfortable swings between hot days and cooler nights. In contrast, the vernacular-inspired building demonstrates effective attenuation of daily temperature extremes, maintaining consistently moderate indoor temperatures with much reduced day–night variability.

During the hottest week, a detailed analysis reveals contrasting temperature dynamics between the two case study buildings and the outdoor environment. The outdoor temperature remains consistently high, fluctuating around 39 to 40 °C, underscoring the severity of the heatwave. The contemporary building shows wide temperature swings, with indoor temperatures varying from approximately 30 °C to peaks exceeding 44 °C,

closely mirroring and sometimes amplifying the outdoor temperature fluctuations. In stark contrast, the bioclimatic building maintains a more stable indoor environment, with temperatures hovering steadily near 35 °C and displaying minimal daily variation. This significant difference stems from the thermo-physical properties of the building envelopes: the bioclimatic structure benefits from materials with high thermal inertia, superior insulation, natural ventilation, and solar shading, which collectively buffer heat transfer and dampen rapid temperature changes. Conversely, the contemporary building's less effective insulation and lower thermal mass allow outdoor temperature spikes to permeate indoors, leading to greater discomfort and increased reliance on mechanical cooling. Thus, the observed temperature difference between the two buildings during this extreme heat event highlights the critical role of building envelope characteristics in regulating indoor thermal comfort.

6.3. Thermal Response of the First Case Study Under Climate Change Scenarios

The graphs below in Figures 13 and 14 illustrate the monthly (left) and daily (right) variations in indoor temperature (operative temperature) for the first case study, projecting changes by the year 2050 under different climate scenarios (SSP1-2.6, SSP2-4.5, SSP3-7.0, SSP5-8.5), and comparing them to the current situation (Present—TMY) and outdoor temperature (Outdoor). Overall, future scenarios predict an increase in indoor temperature compared to the current period, with higher values corresponding to the emission intensity of each scenario (SSP5-8.5 being the most extreme). The SSP scenario curves show a consistent and growing gap compared to the black (present) curve, especially during hot months: summer peak temperatures rise more sharply under high-emission scenarios while remaining systematically lower than outdoor temperatures, which exhibit larger amplitude and sharper peaks.

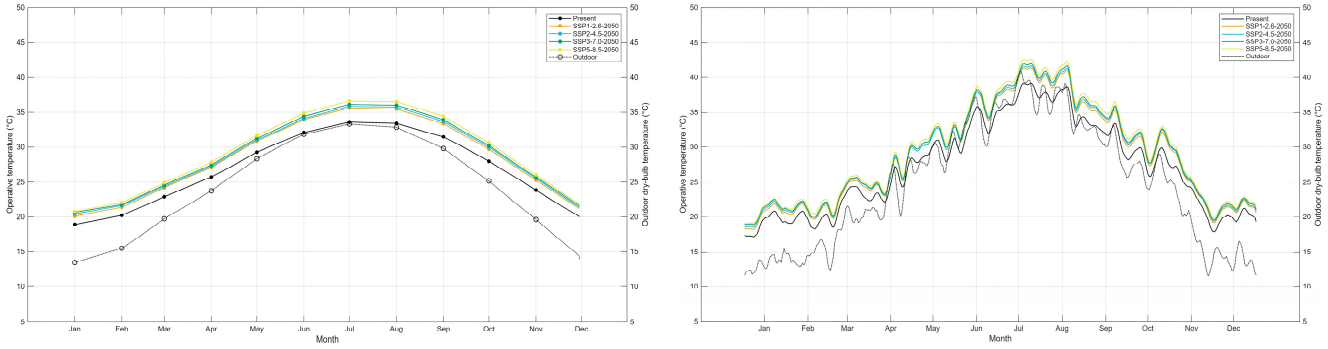

(**a**) (**b**)

Figure 13. Medium-term monthly (**a**) and daily (**b**) internal temperature variations under different scenarios for the first case study.

The daily graph in Figure 13 shows amplified daily differences as well, with indoor temperatures following the chosen climate scenario trend but moderating the sharp outdoor peaks; the hottest days remain hotter in all scenarios compared to the present period. Monthly average indoor temperatures for the first case in 2050 vary roughly between 21 °C in winter (January) and 37 °C in summer (July), with higher peaks for high-emission scenarios. For example, indoor temperature reaches nearly 36.5 °C under SSP5-8.5 in July, while it remains close to 33.5 °C under SSP1-2.6 and about 32 °C for the current situation. The maximum outdoor temperature during this period reaches nearly 45 °C. On the daily variation graph, indoor daily temperatures range roughly from 18 °C to 43 °C depending on the scenario, with peaks corresponding to summer periods and higher for more severe scenarios (SSP5-8.5). Outdoor daily temperature varies more widely between

10 °C and above 45 °C, indicating that despite projected warming, the building still partially moderates thermal extremes.

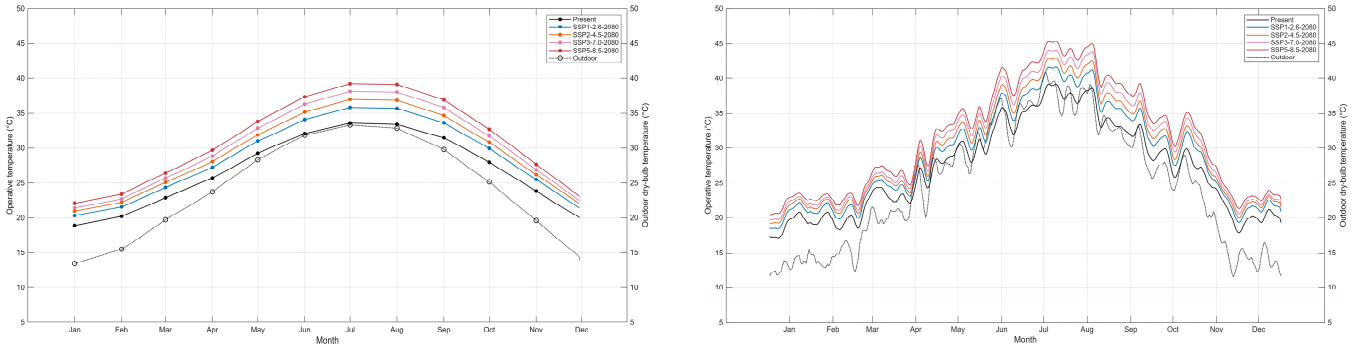

(**a**) (**b**)

Figure 14. Long-term monthly (**a**) and daily (**b**) temperature variations under different scenarios for the first case study.

For the long-term monthly temperature (2080), the graph (Figure 14) shows indoor operative temperatures rising from around 21 °C in winter to nearly 41 °C in summer under the most extreme SSP5-8.5-2080 scenario, while current indoor summer peaks reach about 34 °C. The temperature difference between the mildest scenario SSP1-2.6-2050 and the most severe SSP5-8.5-2080 is approximately 5–6 °C during summer months, with all indoor temperatures remaining below outdoor peaks, which reach about 45 °C. On the daily scale, indoor temperatures consistently increase in all SSP scenarios compared to present-day values, particularly during summer, with peaks exceeding 40 °C under high-emission scenarios, while winter lows stay above 20 °C. The outdoor temperature shows wider fluctuations, from roughly 10 °C in winter to over 45 °C in summer. Overall, although the building moderates extreme outdoor temperatures, it faces increasing thermal stress under future warming, with comfort challenges becoming more pronounced in high emission scenarios.

The comparison between mid-term and long-term results for the first case study shows a clear trend of increasing indoor temperatures as climate scenarios progress from moderate to severe emissions and from 2050 to 2080. In both periods, indoor temperatures rise following the patterns of the respective climate scenarios, with summer peaks becoming more pronounced over time. While the building consistently moderates the sharp temperature fluctuations observed outside, it becomes increasingly challenging to maintain comfortable indoor conditions due to the strengthening thermal stress in higher emission scenarios and later decades. The difference between mid-term and long-term projections highlights a growing gap in indoor thermal conditions, suggesting a heightened risk of overheating and the need for enhanced adaptation measures in the building design and operation as time progresses.

6.4. Thermal Response of the Second Case Study Under Climate Change Scenarios

Figure 15 illustrates both monthly and daily temperature trends for the second case study under different 2050 climate scenarios. The monthly graph shows that indoor operative temperatures consistently stay lower than outdoor temperatures, with indoor summer peaks ranging from about 31 to 33.5 °C across scenarios, compared to outdoor maximums reaching around 34 to 37 °C. Winter indoor temperatures range between approximately 17 and 19 °C, while outdoor lows dip to about 13 to 15 °C. Even in the most severe SSP5-8.5 scenario, indoor temperatures rise only slightly above current conditions, reflecting the building's effective thermal regulation.

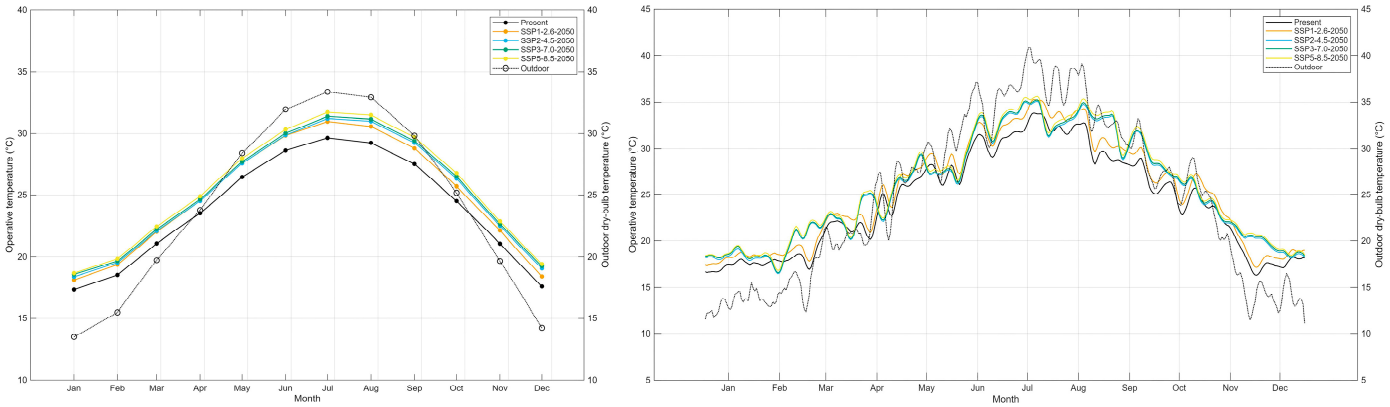

(**a**) (**b**)

Figure 15. Medium-term monthly (**a**) and daily (**b**) temperature variations under different scenarios for the second case study.

The daily graph reveals that indoor temperatures follow climate scenario trends but with notably less fluctuation than the outdoor temperatures, which oscillate between roughly 8 and 42 °C. Indoor daily temperatures vary approximately between 16 and 38 °C depending on the scenario, showing controlled daily peaks especially when compared to outdoor extremes. The building limits sharp temperature spikes, maintaining more stable comfort conditions year-round.

For the long-term monthly temperature projections (2080), the graphs Figure 16, for the second case study demonstrate indoor operative temperatures increasing as climate scenarios become more severe, but the rise remains moderate compared to the outdoors. Under the most extreme scenario (SSP5-8.5-2080), indoor values climb from around 18 °C in winter up to approximately 37 °C in summer, while milder scenarios (e.g., SSP1-2.6) present a narrower range of about 17 °C to 32 °C. In all cases, summer indoor peaks remain substantially below outdoor peaks, which approach 40 °C. The difference between the lowest and highest scenarios indoors during summer months is about 5 °C, smaller than the variation seen outside.

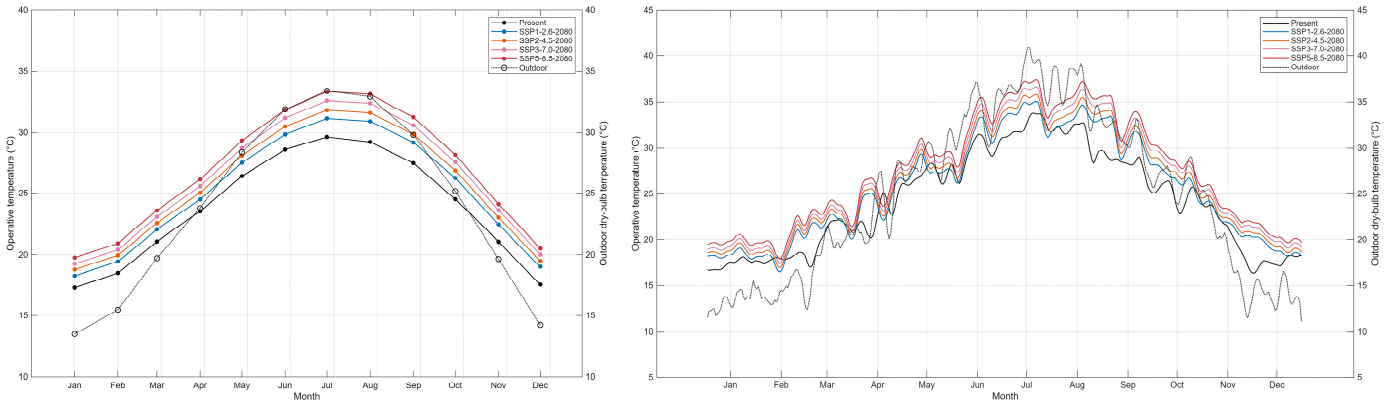

(**a**) (**b**)

Figure 16. Long-term monthly (**a**) and daily (**b**) temperature variations under different scenarios for the second case study.

On the daily scale, indoor temperatures increase in all SSP scenarios compared to current values, mostly during the summer, with the most severe scenario leading to summer peaks near 37 °C. However, even under high emissions, indoor temperatures do not reach outdoor extremes, and winter lows remain well above outdoor minima, typically above

15 °C. Outdoor daily temperatures remain highly variable, from about 10 °C in winter to nearly 40 °C in summer.

Compared to the first case study, the thermal performance shown in the second case study demonstrates a significantly enhanced ability to moderate indoor temperatures, effectively mitigating both seasonal and daily thermal stresses even as climate scenarios become more severe. This difference directly illustrates the critical role of advanced thermo-physical properties in building envelopes, such as increased thermal inertia, optimized insulation, and carefully considered solar protection, in maintaining stable indoor environments under future climate conditions.

The data further highlight that, despite a general warming trend and intensifying projected scenarios, the second case study's envelope consistently buffers indoor conditions: indoor temperatures remain lower than outdoor values, extreme peaks are notably less pronounced, and the annual temperature range narrows. Even under the most severe climate projections, interior comfort conditions do not deteriorate as sharply as observed in less-optimized structures. While it is inevitable that extreme scenarios will challenge comfort, the building's advanced design features especially the combination of high thermal mass, robust insulation, and passive solar control significantly limit the impact of climate change within interior spaces. Overall, this confirms that investing in high-performance envelope technologies provides tangible benefits for occupant comfort and long-term resilience.

6.5. Thermal Comfort and Discomfort Intensity Under the Different Climate Scenarios

In this section, the analysis focuses on the evaluation of thermal comfort in the two buildings studied, based on the adaptive model from the ASHRAE 55-2023 standard applied under natural ventilation conditions. This model establishes a relationship between the comfortable indoor temperature and the mean outdoor temperature, taking into account the gradual adaptation of occupants to climatic variations. According to ASHRAE 55-2023 adaptive comfort model's 90% acceptability limit, indicating ranges of indoor temperatures considered acceptable by 90% of occupants with respect to the prevailing mean outdoor temperature. The comfortable range for operative indoor temperatures generally lies between approximately 21 °C and 27 °C during summer, depending on the mean outdoor temperature, which here varies between 10 °C and 33 °C.

The results presented in Figure 17 detail the comfort band as defined by the adaptive thermal comfort standard, alongside the range of simulated operative temperatures for both current and future periods under the SSP1-2.6-2080 and SSP5-8.5-2080 scenarios, thereby emphasizing the direct influence of climate change trajectories on indoor comfort conditions within contemporary and vernacular constructions. The plotted correlation between prevailing mean outdoor temperature and indoor operative temperature, under natural ventilation, reveals that during the present climate period, a substantial proportion of operative temperatures for contemporary buildings consistently fall above the 80% and 90% comfort intervals, evidencing pronounced thermal discomfort. Vernacular buildings, however, maintain a considerably higher proportion of readings within the comfort zone, reflecting enhanced passive moderation. For the 2080 climate projections, the spread of data points shifts further above the defined comfort bands, particularly under the SSP5-8.5 scenario, with both building types experiencing frequent exceedance of adaptive comfort limits and highlighting a marked escalation in thermal stress. Nonetheless, the vernacular models display less severe departures from the neutral line and a tighter clustering within the adaptive bands, indicating superior resilience and adaptability to increased outdoor temperatures. In contrast, contemporary buildings exhibit higher operative temperatures and greater variability away from the neutral line, underlining their susceptibility to overheating and reduced comfort.

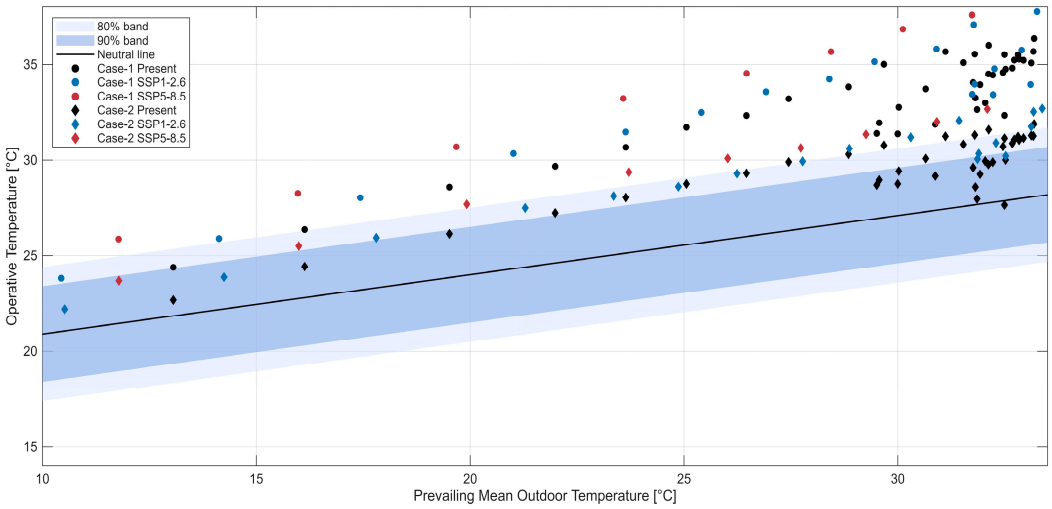

Figure 17. Comparison of adaptive thermal comfort zone and simulated operative temperatures.

Under the present climate scenario (TMY), the results show a clear gap in thermal comfort performance between contemporary and vernacular buildings. The operative temperature readings for contemporary structures often fall beyond the 80% and 90% adaptive comfort intervals, indicating persistent episodes of thermal discomfort and frequent overheating risks. In contrast, vernacular constructions demonstrate a higher concentration of operative temperatures within the prescribed comfort bands.

Looking ahead to the moderate future climate scenario (SSP1-2.6, 2080), both building types experience a marked shift towards elevated operative temperatures, with contemporary models frequently surpassing the adaptive comfort thresholds. This trend signifies a substantial increase in the frequency and severity of thermal discomfort events. Despite this deterioration, vernacular buildings retain a measurable advantage, with a higher proportion of temperature points clustering within the comfort zone though the margin of safety is reduced as external warming intensifies.

The severe future scenario (SSP5-8.5, 2080) presents the greatest challenge to indoor comfort. Operative temperatures rise dramatically across both building types, and the majority of readings for contemporary buildings and a significant portion for vernacular constructions fall well above the adaptive comfort limits. Overheating episodes become frequent and intense, posing major risks to occupant well-being. Vernacular solutions still outperform their contemporary counterparts by displaying smaller deviations from the neutral zone and maintaining a more compact clustering within the adaptive band, though the extreme context nonetheless exposes the limits of passive moderation. Scholarly consensus supports the observation that vernacular strategies afford inherent resilience to thermal stress, but their capacity to safeguard comfort diminishes rapidly in the face of severe climate change.

To quantify the level of thermal comfort related to indoor air temperature, the index I_{sum} has been defined as a measure of thermal discomfort during the summer season within an indoor environment. This parameter represents the integrated discomfort over a specified period, and by definition, thermal comfort improves as the value of I_{sum} decreases and approaches zero. In this study, with a focus on summer comfort, the I_{sum} index (Equation (5)) is applied using a formula consistent with those employed in previous research [89,96,97]. The reference comfort temperature T_h is set at 27 °C, the time step is fixed at one hour, and 2207 corresponds to the total number of hours covering the summer period from 1 June to 31 August. The detailed results of this analysis will be presented in Table 4.

Table 4. Thermal Discomfort under Current (TMY), SSP1-2.6 and SSP5-8.5 future Scenarios.

Case	Scenarios	Discomfort Index	
		Adaptive Model (Hours/2207)	Integrated Summer Degree (°C·h)
Contemporary building (first case study)	Current performance (TMY)	2110	17,002.3
	Best performance under SSP1-2.6-2080	2122	21,398.7
	Worst performance under SSP5-8.5-2080	2124	28,511.5
Vernacular building (second case study)	Current performance (TMY)	1638	8206.5
	Best performance under SSP1-2.6-2080	1827	11,171.2
	Worst performance under SSP5-8.5-2080	2011	15,559.0

Table 4 provides a comprehensive examination of thermal discomfort hours experienced within two distinct building types, namely a contemporary building and a vernacular building, across three climate scenarios: the Typical Meteorological Year (TMY), which represents current climatic conditions, and a projected best-case future scenario following SSP1-2.6 for the year 2080 and finally the worst-case future scenario following SSP5-8.5 for the year 2080.

Under the present climate, the contemporary building exhibits considerably elevated levels of discomfort, as evidenced by an I_{sum} value of 17,002.3 °C·h and 2110 h during which indoor temperatures exceed 27 °C under the present scenario (TMY). Conversely, the vernacular building demonstrates superior thermal resilience, recording I_{sum} values of 8206.5 and 1638 discomfort hours. In other words, the vernacular building exhibits approximately 22% fewer discomfort hours than the contemporary building, and its integrated summer discomfort degree I_{sum} is almost half that of the contemporary case. This reflects the stronger moderating effect of the vernacular envelope, which combines heavier walls, higher thermal mass and more effective solar control.

Under the best-case future scenario SSP1-2.6, discomfort still increases in both buildings. For the contemporary one, Isum rises by 25.8%, while adaptive discomfort exceedance hours increase only marginally by 0.6%. For the vernacular building, discomfort hours increase by 11.5% and Isum by 36.1%. Despite its deterioration, the vernacular case still accumulates only about half of the overheating degree-hours of the contemporary building.

Under the most severe future scenario SSP5-8.5 by late century, the performance of both buildings degrades substantially. The vernacular dwelling still outperforms the contemporary one in absolute terms, but the overheating burden increases markedly in both cases. Relative to the present climate, Isum rises by about 89.6% for the vernacular case and 67.7% for the contemporary case. These results indicate that, although the vernacular strategy remains more resilient, neither building can maintain acceptable summer comfort under the projected late-century hot–arid conditions without additional adaptation measures.

From a design and retrofit perspective, these findings suggest that vernacular-inspired envelope strategies offer a more robust baseline for hot–arid cities, but they are not sufficient on their own under high-emission futures. Future interventions in similar contexts should therefore combine envelope-oriented measures with low-energy active strategies, in order to limit overheating and maintain acceptable comfort levels across the range of projected climate scenarios. Key factors include the deliberate selection of materials, utilization of thermal mass, enhanced insulation, and passive cooling methods such as nocturnal ventilation. The materials to be selected encompass traditional, locally sourced earth-based

components stabilized earth, adobe bricks, rammed earth, and stone with high thermal inertia, moderating indoor temperatures by absorbing heat during the day and releasing it overnight. Selection criteria prioritize these materials based on thermal mass, durability, local availability, and cultural appropriateness. Acknowledging practical limitations of traditional materials, modern alternatives like advanced composites, stabilized earth blocks, lightweight concrete, and insulated panels are also incorporated, replicating key thermal properties whilst conforming to contemporary structural and sustainability requirements.

The remarkable ability of the vernacular building to reduce temperature fluctuations both between day and night and among different rooms can be directly attributed to the thermal properties and configuration of its construction materials, as summarized in Table 1. The primary walls, composed of lime-sandstone with a high density and substantial thermal capacity, are notably thick, resulting in significant thermal mass. This high thermal mass enables the walls to absorb and store heat during the day, releasing it slowly at night, thereby buffering rapid temperature swings and stabilizing the indoor climate. Furthermore, the wall's relatively low heat transfer coefficient restricts heat exchange between the building's interior and the external environment, providing further moderation of interior conditions. Similarly, the layered roof assembly including granite tile, cement, and hollow concrete blocks combines dense materials, each contributing to overall thermal inertia.

This configuration delays heat penetration during the hottest periods and tempers nocturnal heat loss, with the internal plaster layer providing additional resistance to sudden thermal changes. The roof's global heat transfer coefficient complements this effect, balancing delayed heat gain by day and promoting gradual cooling at night. Additionally, the deliberate spatial distribution of rooms, as well as the inclusion of passive ventilation features such as the wind catcher (malqaf), enhance cross-ventilation and promote convective cooling, further evening out thermal gradients throughout the building. In combination, these vernacular design strategies thick, high-mass envelope construction, layered roof assembly, optimized room arrangement, and integrated passive cooling devices confer the ability to maintain milder daily and nightly temperature swings across rooms.

7. Conclusions

This paper highlights the crucial importance of integrating climate sensitive vernacular architectural strategies into the design of residential buildings in hot and arid regions to address the growing impacts of climate change. Through dynamic thermal simulations under current and future climate scenarios, the results show that vernacular-inspired buildings consistently outperform contemporary models in mitigating thermal discomfort and overheating, even in the face of significant increases in future temperatures. While both building types experience increased thermal stress under future warming, vernacular designs offer a significant advantage by reducing overheating degree. For example, simulations indicate that during the hottest projected summers in 2080, indoor temperatures in bioclimatic buildings reach approximately 37 °C, compared to 41 °C in extreme scenarios for less efficient buildings, with outdoor temperatures exceeding 45 °C.

The comparison between contemporary and vernacular buildings reveals a clear superiority of the latter in terms of passive capabilities to moderate thermal variations and reduce energy consumption, demonstrated by a significantly higher percentage of comfort hours under critical thresholds (e.g., nearly 87% of hours below 33 °C for vernacular buildings versus less than 20% for contemporary buildings under current conditions). This resilience is attributed to passive design strategies inherent in vernacular architecture, such as enhanced shading, natural ventilation potential, and thermal mass optimization, which collectively limit indoor heat accumulation.

The study of the integrated discomfort degrees shows that contemporary building presents significantly higher discomfort, unlike the vernacular building, which demonstrates better thermal performance under both TMY and future conditions. Although discomfort increases for both types under the effect of future warming, vernacular design consistently reduces thermal stress compared to contemporary construction. This persistent gap highlights the inherent capacity of the vernacular building to limit heat accumulation and maintain better thermal comfort, even in the face of intensifying climatic challenges. The results clearly indicate that, although both building types of experience increased thermal discomfort due to future warming, vernacular architecture, through its design principles and traditional materials, offers a robust adaptation strategy that mitigates heat stress more effectively.

Through the combination of these elements, it is possible to create resilient and energy efficient habitats capable of maintaining occupant comfort and mitigating energy consumption amid rising temperatures and more frequent extreme climatic events. This aligns with broader findings showing a sharp increase in indoor overheating linked to climate change, especially under a severe scenario like SSP5-8.5. Although high thermal resistance and wall inertia can initially reduce overheating, this benefit decreases over time even in well-insulated buildings, reinforcing the need to focus on evolving summer comfort standards to curb escalating air conditioning demands in urban environments.

This study provides a focused and contextually comprehensive assessment, yet several limitations must be acknowledged. The work evaluates two residential buildings, a contemporary apartment and a vernacular-inspired dwelling, whose contrasting envelope characteristics yield valuable insights but do not represent the full diversity of housing typologies. Although the results demonstrate clear differences in thermal resilience between the two cases, particularly the reduced diurnal temperature amplitude and substantially lower overheating exposure observed in the vernacular building, broader generalization would require examining a wider set of archetypes and construction systems. Furthermore, the analysis relies on operative temperature and discomfort degree-hours as primary indicators. These metrics were chosen to isolate the passive thermal behavior of the envelope, which the results confirm as the dominant driver of indoor temperatures under free-running conditions. While this allows a controlled comparison, evident in the vernacular dwelling's marked reductions in overheating and more stable thermal response, future assessments would benefit from integrating additional performance metrics such as heating and cooling energy needs or CO_2 emissions, especially when mechanical systems and occupancy-related internal gains come into play.

Another limitation relies on the model calibration; for the contemporary building it was based on a four-day measurement campaign. Despite the short duration, the simulated and measured temperatures showed excellent agreement, with MBE values within $\pm 0.2\%$, cvRMSE below 1%, and R^2 between 0.86 and 0.89, meeting the accuracy criteria commonly recommended in building performance validation. This confirms that the model reliably captures the envelope-driven thermal dynamics relevant to the study's purpose. Nonetheless, such a brief dataset cannot fully represent seasonal climatic variability, and this limitation introduces uncertainty when extending simulations to future climate scenarios. The study addresses this partly by using multiple independent climate files for 2050 and 2080 and by focusing on comparative trends rather than exact absolute predictions. Even so, longer measurement periods and explicit uncertainty quantification, such as sensitivity analysis or probabilistic calibration, would strengthen future projections.

Finally, it should be noted that the simulations represent unoccupied, free-running conditions. This means that internal gains, occupant behaviour, adaptive actions and HVAC system dynamics were intentionally excluded in order to isolate the effects of the building

envelope. While this approach aligns with the study's objectives and is supported by the strong envelope–temperature correlations observed, complete representations of real-world operation will require incorporating these additional factors in future work. Expanding the range of climates, building parameters, and adaptive strategies would further improve the robustness and generalizability of the findings, particularly as residential buildings face increasing thermal stress under shifting climatic conditions.

Author Contributions: Conceptualization, K.A., S.O. and S.D.T.; methodology, K.A. and S.D.; software, K.A. and S.O.; validation, K.A., S.O. and R.S.; formal analysis, S.O.; investigation, K.A. and S.O.; resources K.A. and S.O.; data curation, I.R.; writing—original draft preparation, K.A., S.O. and S.D.; writing—review and editing, K.A., R.S., S.D.T. and F.R.; visualization, S.D. and I.R.; supervision, F.R. and S.D.T.; project administration, K.A.; funding acquisition, F.R. All authors have read and agreed to the published version of the manuscript.

Funding: This research received no external funding.

Data Availability Statement: The original contributions presented in this study are included in the article. Further inquiries can be directed to the corresponding author.

Acknowledgments: The authors gratefully acknowledge the BERlab and LACOMOFA Laboratories at the University of Biskra for their support with instrumentation, and the Department of Architecture, Construction, and Design at the University of Bari, Italy, for providing access to the simulation software used in this research. The authors also express their sincere appreciation for the valuable assistance received during the experimental work and the scientific stay at the Department.

Conflicts of Interest: The authors declare no conflicts of interest.

Abbreviations

The following abbreviations are used in this manuscript:

I_{sum}	Integrated Discomfort Degree in Summer (°C·h)
SSP	Socioeconomic Scenario Pathways
CC	Climate change
RCM	Regional Climate Model
RCP	Representative Concentration Pathway
CMIP	Coupled Model Intercomparison Project
IPCC	Intergovernmental Panel on Climate Change
SRESs	Special Report on Emissions Scenarios
GCMs	General Circulation Models

References

1. Jung, Y.; Heo, Y.; Lee, H. Multi-objective optimization of the multi-story residential building with passive design strategy in South Korea. *Build. Environ.* **2021**, *203*, 108061. [CrossRef]
2. Duan, Z.; De Wilde, P.; Attia, S.; Zuo, J. Challenges in predicting the impact of climate change on thermal building performance through simulation: A systematic review. *Appl. Energy* **2025**, *382*, 125331. [CrossRef]
3. United Nations. *Report of the United Nations Environment Assembly of the United Nations Environment Programme*; United Nations: New York, NY, USA, 2021.
4. Yong, Z.; Yuan, L.-J.; Qian, Z.; Sun, X.-Y. Multi-objective optimization of building energy performance using a particle swarm optimizer with less control parameters. *J. Build. Eng.* **2020**, *32*, 101505. [CrossRef]
5. Kim, K.-H.; Kabir, E.; Ara Jahan, S. A Review of the Consequences of Global Climate Change on Human Health. *J. Environ. Sci. Health Part C* **2014**, *32*, 299–318. [CrossRef] [PubMed]
6. Boumlik, K.; Belarbi, R.; Ahachad, M.; Mahdaoui, M.; Radoine, H.; Krarti, M. Design Optimization of Energy-Efficient Residential Buildings in Morocco. *Buildings* **2024**, *14*, 3915. [CrossRef]
7. Hinkle, L.E.; Wang, J.; Brown, N.C. Quantifying potential dynamic façade energy savings in early design using constrained optimization. *Build. Environ.* **2022**, *221*, 109265. [CrossRef]

8. Resende, J.; Corvacho, H. Optimisation of Nearly Zero Energy Building Envelope for Passive Thermal Comfort in Southern Europe. *Buildings* **2024**, *14*, 2757. [CrossRef]
9. Albatayneh, A. Optimising the Parameters of a Building Envelope in the East Mediterranean Saharan, Cool Climate Zone. *Buildings* **2021**, *11*, 43. [CrossRef]
10. Di Turi, S.; Ronchetti, L.; Sannino, R. Towards the objective of Net ZEB: Detailed energy analysis and cost assessment for new office buildings in Italy. *Energy Build.* **2023**, *279*, 112707. [CrossRef]
11. Sannino, R.; Ronchetti, L.; Di Turi, S. Pathway to Zero-Emission Buildings: Energy and Economic Comparison of Different Demand Coverage by RES for a New Office Building. *Sustainability* **2024**, *16*, 10837. [CrossRef]
12. Bensayah, A.; Bencheikh, H.; Abdessemed, A. Mzabite Heritage in Southern Algeria: What Bioclimatic Lessons can Be Learned to Optimize Thermal Comfort? In *MATEC Web of Conferences*; EDP Sciences: Les Ulis, France, 2019; Volume 278, p. 04005. [CrossRef]
13. Halicioglu, F.H. Analysis of vernacular architecture in terms of sustainable considerations: The case of şirince village in western turkey. *Int. J. Sustain. Trop. Des. Res. Pract.* **2012**, *5*, 39–54.
14. Beccali, M.; Strazzeri, V.; Germanà, M.L.; Melluso, V.; Galatioto, A. Vernacular and bioclimatic architecture and indoor thermal comfort implications in hot-humid climates: An overview. *Renew. Sustain. Energy Rev.* **2018**, *82*, 1726–1736. [CrossRef]
15. Khelifi, L. Re-evaluating Vernacular Climatic Morphologies for Sustainable Development in Southern Algeria. In *E3S Web of Conferences*; EDP Sciences: Les Ulis, France, 2024; Volume 585, p. 01023. [CrossRef]
16. Toroxel, J.L.; Silva, S.M. A Review of Passive Solar Heating and Cooling Technologies Based on Bioclimatic and Vernacular Architecture. *Energies* **2024**, *17*, 1006. [CrossRef]
17. Duraković, B. Passive Solar Heating/Cooling Strategies. In *PCM-Based Building Envelope Systems*; Springer International Publishing: Cham, Switzerland, 2020; pp. 39–62.
18. Matari, N.; Mahi, A.; Chabane, N.; Harrat, Z.R.; Hadzima-Nyarko, M. Design Methodology Development for High-Energy-Efficiency Buildings in Algerian Sahara Climatic Context. *Sustainability* **2025**, *17*, 2660. [CrossRef]
19. Stasi, R.; Ruggiero, F.; Berardi, U. From Energy-Intensive Buildings to NetPlus Targets: An Innovative Solar Exoskeleton for the Energy Retrofitting of Existing Buildings. *Energy Build.* **2025**, *333*, 115416. [CrossRef]
20. Hu, M. Exploring Low-Carbon Design and Construction Techniques: Lessons from Vernacular Architecture. *Climate* **2023**, *11*, 165. [CrossRef]
21. Zong, J.; Wan Mohamed, W.S.; Zaky Jaafar, M.F.; Ujang, N. Sustainable development of vernacular architecture: A systematic literature review. *J. Asian Archit. Build. Eng.* **2025**, *24*, 3558–3574. [CrossRef]
22. Abdel Gelil Mohamed, N.; Abo Eldardaa Mahmoud, I. Cost-effectiveness and affordability evaluation of a residential prototype built with compressed earth bricks, hybrid roofs and palm midribs. *Front. Built Environ.* **2023**, *9*, 1058782. [CrossRef]
23. Ben Charif, H.; Belakehal, A.; Zerari, S. Earthen Architecture in Southern Algeria: An Assessment of Social Values and the Impact of Industrial Building Practices. *Open Archaeol.* **2023**, *9*, 20220324. [CrossRef]
24. Hailu, H.; Gelan, E.; Girma, Y. Indoor Thermal Comfort Analysis: A Case Study of Modern and Traditional Buildings in Hot-Arid Climatic Region of Ethiopia. *Urban Sci.* **2021**, *5*, 53. [CrossRef]
25. Chandel, S.S.; Sharma, V.; Marwah, B.M. Review of energy efficient features in vernacular architecture for improving indoor thermal comfort conditions. *Renew. Sustain. Energy Rev.* **2016**, *65*, 459–477. [CrossRef]
26. Makris, D.; Antzoulatou, A.; Romaios, A.; Malefaki, S.; Paravantis, J.A.; Giannadakis, A.; Mihalakakou, G. Optimizing Energy and Cost Performance in Residential Buildings: A Multi-Objective Approach Applied to the City of Patras, Greece. *Energies* **2025**, *18*, 3361. [CrossRef]
27. Lotfabadi, P.; Hançer, P. A Comparative Study of Traditional and Contemporary Building Envelope Construction Techniques in Terms of Thermal Comfort and Energy Efficiency in Hot and Humid Climates. *Sustainability* **2019**, *11*, 3582. [CrossRef]
28. Pardo, J.M.F. Challenges and Current Research Trends for Vernacular Architecture in a Global World: A Literature Review. *Buildings* **2023**, *13*, 162. [CrossRef]
29. Kaihoul, A.; Sriti, L.; Amraoui, K.; Di Turi, S.; Ruggiero, F. The effect of climate-responsive design on thermal and energy performance: A simulation based study in the hot-dry Algerian South region. *J. Build. Eng.* **2021**, *43*, 103023. [CrossRef]
30. Moscoso-García, P.; Quesada-Molina, F. Analysis of Passive Strategies in Traditional Vernacular Architecture. *Buildings* **2023**, *13*, 1984. [CrossRef]
31. Kubota, T.; Zakaria, M.A.; Abe, S.; Toe, D.H.C. Thermal functions of internal courtyards in traditional Chinese shophouses in the hot-humid climate of Malaysia. *Build. Environ.* **2017**, *112*, 115–131. [CrossRef]
32. Salameh, M.; Touqan, B. Traditional Passive Design Solutions as a Key Factor for Sustainable Modern Urban Designs in the Hot, Arid Climate of the United Arab Emirates. *Buildings* **2022**, *12*, 1811. [CrossRef]
33. Bagasi, A.A.; Calautit, J.K. Experimental field study of the integration of passive and evaporative cooling techniques with Mashrabiya in hot climates. *Energy Build.* **2020**, *225*, 110325. [CrossRef]
34. Fardous, I.A.S. *Adaptation of an Architectonic Tradition for a Sustainable Future in the Middle East: A Case Study of Three Building Typologies in Riyadh City*; Robert Gordon University: Aberdeen, UK, 2020.

35. Handayani Lubis, I.; Donny Koerniawan, M.; Budiarto, R. The Application of Traditional Architecture as Passive Design Strategies for Modern Architecture in Hot Dry Climate. In *IOP Conference Series: Materials Science and Engineering*; IOP Publishing: Bristol, UK, 2018; Volume 401, p. 012004. [CrossRef]
36. Sözer, H.; Bekele, S. Evaluation of innovative sustainable design techniques from traditional architecture: A case study for the cold dry climatic region in Turkey. *Archit. Sci. Rev.* **2018**, *61*, 143–155. [CrossRef]
37. VILALTA Completes Mall in Ethiopia with Perforated Envelope. Designboom | Architecture & Design Magazine. 2016. Available online: https://www.designboom.com/architecture/vilalta-arquitectura-lideta-mercato-shopping-mall-addis-ababa-ethiopia-12-26-2016/ (accessed on 28 October 2025).
38. Kaihoul, A.; Pitzalis, E.; Sriti, L.; Di Turi, S.; Amraoui, K. Enhancing thermal comfort assessment: A sensitivity study of PMV-PPD and adaptive models in an Algerian reference hotel across different climate zones. *Indoor Built Environ.* **2024**, *33*, 1680–1704. [CrossRef]
39. Berbouche, C.; Sriti, L.; Latreche, S. Vernacular Features in Rural Housing of the Aurassien massif between Traditional Practices and Bioclimatic Aspect. Case study of Ain Zaatout (Algeria). *Tech. Soc. Sci. J.* **2023**, *39*, 730–741. [CrossRef]
40. Bencheikh, D.; Bederina, M. Assessing the duality of thermal performance and energy efficiency of residential buildings in hot arid climate of Laghouat, Algeria. *Int. J. Energy Environ. Eng.* **2020**, *11*, 143–162. [CrossRef]
41. Daoudi, N.S.; Mestoul, D.; Lamraoui, S.; Boussoualim, A.; Adolphe, L.; Bensalem, R. Vernacular Architecture in Arid Climates: Adaptation to Climate Change. In *Bioclimatic Architecture in Warm Climates*; Guedes, M.C., Cantuaria, G., Eds.; Springer International Publishing: Cham, Switzerland, 2019; pp. 119–154.
42. Diafat, A.; Madani, S. Tafilalt in the Mzab Valley—Algeria. A sustainable urban project in arid environment. *Urbe Rev. Bras. Gestão Urbana* **2019**, *11*, e20190023. [CrossRef]
43. Arigue, B.; Sriti, L.; Santi, G.; Khadraoui, M.A.; Bencheikh, D. Exploring the Cooling Potential of Ventilated Mask Walls in Neo-Vernacular Architecture: A Case Study of André Ravéreau's Dwellings in M'zab Valley, Algeria. *Buildings* **2023**, *13*, 837. [CrossRef]
44. Kaihoul, A.; El Youssef, M.; Pitzalis, E.; Sriti, L.; Dechouk, Y.; Amraoui, K.; Khelil, A.E. Optimising Thermal Comfort in Algerian Reference Hotel Across Eight Climate Zones: A Comparative Study of Simulation and Psychrometric Chart Results. *Sustainability* **2025**, *17*, 6249. [CrossRef]
45. Khechiba, A.; Djaghrouri, D.; Benabbas, M.; Leccese, F.; Rocca, M.; Salvadori, G. Balancing Thermal Comfort and Energy Consumption in Residential Buildings of Desert Areas: Impact of Passive Strategies. *Sustainability* **2023**, *15*, 8383. [CrossRef]
46. Aljawad, R.H. Thermal performance analysis of local building materials for energy efficiency in Iraq. *J. Therm. Eng.* **2024**, *10*, 1011–1020. [CrossRef]
47. Semahi, S.; Benbouras, M.A.; Mahar, W.A.; Zemmouri, N.; Attia, S. Development of Spatial Distribution Maps for Energy Demand and Thermal Comfort Estimation in Algeria. *Sustainability* **2020**, *12*, 6066. [CrossRef]
48. Alalouch, C.; Al-Saadi, S.; AlWaer, H.; Al-Khaled, K. Energy saving potential for residential buildings in hot climates: The case of Oman. *Sustain. Cities Soc.* **2019**, *46*, 101442. [CrossRef]
49. Djeddou, B.; Daich, S.; Femmam, A. The impact of urban form on the energy efficiency of residential buildings in a hot climate. Case study: Ouargla city. *J. Build. Phys.* **2025**, *48*, 821–849. [CrossRef]
50. Iftikhar, S.H.; Anwar, A.; Razzaq, M. Comparative Analysis of the Thermal Performance of a Traditional and a Contemporary House: A Case Study of Abbottabad City. *Glob. Reg. Rev.* **2022**, *VII*, 193–208. [CrossRef]
51. Amraoui, K.; Sriti, L.; Di Turi, S.; Ruggiero, F.; Kaihoul, A. Exploring building's envelope thermal behavior of the neo-vernacular residential architecture in a hot and dry climate region of Algeria. *Build. Simul.* **2021**, *14*, 1567–1584. [CrossRef]
52. Lotfi, Y.; Hassan, M. Optimizing energy efficiency and thermal comfort of green envelope applications in hot arid climate. *Discov. Appl. Sci.* **2024**, *6*, 66. [CrossRef]
53. Daich, S.; Saadi, M.Y.; Santoro, A.; Piras, F.; Boumaraf, B. Spatiotemporal analysis, monitoring, and future prediction of land use/land cover changes in Ghouts: A sustainable agricultural system in the El Oued Oases, Algeria. *Environ. Monit. Assess.* **2025**, *197*, 1062. [CrossRef]
54. Stasi, R.; Ruggiero, F.; Berardi, U. Natural ventilation effectiveness in low-income housing to challenge energy poverty. *Energy Build.* **2024**, *304*, 113836. [CrossRef]
55. Asimakopoulos, D.A.; Santamouris, M.; Farrou, I.; Laskari, M.; Saliari, M.; Zanis, G.; Giannakidis, G.; Tigas, K.; Kapsomenakis, J.; Douvis, C.; et al. Modelling the energy demand projection of the building sector in Greece in the 21st century. *Energy Build.* **2012**, *49*, 488–498. [CrossRef]
56. Nik, V.M.; Sasic Kalagasidis, A. Impact study of the climate change on the energy performance of the building stock in Stockholm considering four climate uncertainties. *Build. Environ.* **2013**, *60*, 291–304. [CrossRef]
57. Shibuya, T.; Croxford, B. The effect of climate change on office building energy consumption in Japan. *Energy Build.* **2016**, *117*, 149–159. [CrossRef]

58. Hwang, R.-L.; Lin, C.-Y.; Huang, K.-T. Spatial and temporal analysis of urban heat island and global warming on residential thermal comfort and cooling energy in Taiwan. *Energy Build.* **2017**, *152*, 804–812. [CrossRef]
59. Mata, É.; Wanemark, J.; Nik, V.M.; Sasic Kalagasidis, A. Economic feasibility of building retrofitting mitigation potentials: Climate change uncertainties for Swedish cities. *Appl. Energy* **2019**, *242*, 1022–1035. [CrossRef]
60. Moazami, A.; Nik, V.M.; Carlucci, S.; Geving, S. Impacts of future weather data typology on building energy performance—Investigating long-term patterns of climate change and extreme weather conditions. *Appl. Energy* **2019**, *238*, 696–720. [CrossRef]
61. Silvero, F.; Lops, C.; Montelpare, S.; Rodrigues, F. Impact assessment of climate change on buildings in Paraguay—Overheating risk under different future climate scenarios. *Build. Simul.* **2019**, *12*, 943–960. [CrossRef]
62. Berardi, U.; Jafarpur, P. Assessing the impact of climate change on building heating and cooling energy demand in Canada. *Renew. Sustain. Energy Rev.* **2020**, *121*, 109681. [CrossRef]
63. Haddad, S.; Barker, A.; Yang, J.; Kumar, D.I.M.; Garshasbi, S.; Paolini, R.; Santamouris, M. On the potential of building adaptation measures to counterbalance the impact of climatic change in the tropics. *Energy Build.* **2020**, *229*, 110494. [CrossRef]
64. Perera, A.T.D.; Nik, V.M.; Chen, D.; Scartezzini, J.-L.; Hong, T. Quantifying the impacts of climate change and extreme climate events on energy systems. *Nat. Energy* **2020**, *5*, 150–159. [CrossRef]
65. Stagrum, A.E.; Andenæs, E.; Kvande, T.; Lohne, J. Climate Change Adaptation Measures for Buildings—A Scoping Review. *Sustainability* **2020**, *12*, 1721. [CrossRef]
66. Nguyen, A.T.; Rockwood, D.; Doan, M.K.; Dung Le, T.K. Performance assessment of contemporary energy-optimized office buildings under the impact of climate change. *J. Build. Eng.* **2021**, *35*, 102089. [CrossRef]
67. Calama-González, C.M.; Suárez, R.; León-Rodríguez, Á.L. Thermal comfort prediction of the existing housing stock in southern Spain through calibrated and validated parameterized simulation models. *Energy Build.* **2022**, *254*, 111562. [CrossRef]
68. Salvati, A.; Kolokotroni, M. Generating future-urban weather files for building performance simulations: Case studies in London. In Proceedings of the 2021 Building Simulation Conference, Bruges, Belgium, 1–3 September 2021.
69. Tootkaboni, M.P.; Ballarini, I.; Zinzi, M.; Corrado, V. A Comparative Analysis of Different Future Weather Data for Building Energy Performance Simulation. *Climate* **2021**, *9*, 37. [CrossRef]
70. Hosseini, M.; Javanroodi, K.; Nik, V.M. High-resolution impact assessment of climate change on building energy performance considering extreme weather events and microclimate—Investigating variations in indoor thermal comfort and degree-days. *Sustain. Cities Soc.* **2022**, *78*, 103634. [CrossRef]
71. Kazanci, O.B.; Shinoda, J.; Olesen, B.W. Revisiting radiant cooling systems from a resiliency perspective: A preliminary study. In Proceedings of the CLIMA 2022 Conference, Rotterdam, The Netherland, 22–25 May 2022. [CrossRef]
72. Rahif, R.; Norouziasas, A.; Elnagar, E.; Doutreloup, S.; Pourkiaei, S.M.; Amaripadath, D.; Romain, A.-C.; Fettweis, X.; Attia, S. Impact of climate change on nearly zero-energy dwelling in temperate climate: Time-integrated discomfort, HVAC energy performance, and GHG emissions. *Build. Environ.* **2022**, *223*, 109397. [CrossRef]
73. Machard, A.; Inard, C.; Alessandrini, J.M.; Devys-Peyre, F.; Martinez, S.; Ribéron, J.; Pelé, C. Climate change influence on buildings dynamic thermal behavior during summer overheating periods: An in-depth sensitivity analysis. *Energy Build.* **2023**, *284*, 112758. [CrossRef]
74. Rodrigues, E.; Fernandes, M.S.; Carvalho, D. Future weather generator for building performance research: An open-source morphing tool and an application. *Build. Environ.* **2023**, *233*, 110104. [CrossRef]
75. Qian, B.; Yu, T.; Zhang, C.; Heiselberg, P.; Lei, B.; Yang, L. A method of determining typical meteorological year for evaluating overheating performance of passive buildings. *Build. Simul.* **2023**, *16*, 511–526. [CrossRef]
76. Park, J.; Lee, K.H.; Lee, S.H.; Hong, T. Benefits assessment of cool skin and ventilated cavity skin: Saving energy and mitigating heat and grid stress. *Build. Environ.* **2024**, *247*, 111027. [CrossRef]
77. Wehbi, H.; Messadi, T. Challenges That Impact the Development of a Multi-Generational Low-Carbon Passive House in a Small City. *Designs* **2024**, *8*, 52. [CrossRef]
78. Hostein, M.; Musy, M.; Moujalled, B.; El Mankibi, M. Generating meteorological files of future climates with heatwaves in urban context to evaluate building overheating: An energy-efficient dwelling case study. *Build. Environ.* **2024**, *263*, 111874. [CrossRef]
79. Mulverhill, C.; Coops, N.C.; Wulder, M.A.; Hermosilla, T.; White, J.C.; Bater, C.W. Projected Future Changes in Burn Probability in Canada's Forests and Communities Under Different Climate Change Scenarios. *Can. J. Remote Sens.* **2025**, *51*, 2560347. [CrossRef]
80. CMIP Overview—Coupled Model Intercomparison Project. 2023. Available online: https://wcrp-cmip.org/cmip-overview/#:~:text=The%20Coupled%20Model%20Intercomparison%20Project%20(CMIP)%20is%20an,code%20that%20creates%20a%20digital%20analogue%20to%20Earth (accessed on 18 September 2025).
81. Meehl, G.A.; Boer, G.J.; Covey, C.; Latif, M.; Stouffer, R.J. The coupled model intercomparison project (CMIP). *Bull. Am. Meteorol. Soc.* **2000**, *81*, 313–318. [CrossRef]
82. Lee, H.; Calvin, K.; Dasgupta, D.; Krinner, G.; Mukherji, A.; Thorne, P.; Trisos, C.; Romero, J.; Aldunce, P.; Barrett, K.; et al. *Climate Change 2023: Synthesis Report. Contribution of Working Groups I, II and III to the Sixth Assessment Report of the Intergovernmental Panel on Climate Change*; IPCC: Geneva, Switzerland, 2023.

83. Allan, R.P.; Arias, P.A.; Berger, S.; Canadell, J.G.; Cassou, C.; Chen, D.; Cherchi, A.; Connors, S.L.; Coppola, E.; Cruz, F.A. Intergovernmental panel on climate change (IPCC). Summary for policymakers. In *Climate Change 2021: The Physical Science Basis. Contribution of Working Group I to the Sixth Assessment Report of the Intergovernmental Panel on Climate Change*; Cambridge University Press: Cambridge, UK, 2023; pp. 3–32.
84. Nakicenovic, N.; Alcamo, J.; Davis, G.; Vries, B.D.; Fenhann, J.; Gaffin, S.; Gregory, K.; Grubler, A.; Jung, T.Y.; Kram, T. *Special Report on Emissions Scenarios*; Lawrence Berkeley National Laboratory: Berkeley, CA, USA, 2000.
85. Van Vuuren, D.P.; Edmonds, J.; Kainuma, M.; Riahi, K.; Thomson, A.; Hibbard, K.; Hurtt, G.C.; Kram, T.; Krey, V.; Lamarque, J.-F. The representative concentration pathways: An overview. *Clim. Change* **2011**, *109*, 5. [CrossRef]
86. O'Neill, B.C.; Kriegler, E.; Riahi, K.; Ebi, K.L.; Hallegatte, S.; Carter, T.R.; Mathur, R.; Van Vuuren, D.P. A new scenario framework for climate change research: The concept of shared socioeconomic pathways. *Clim. Change* **2014**, *122*, 387–400. [CrossRef]
87. Riahi, K.; Van Vuuren, D.P.; Kriegler, E.; Edmonds, J.; O'Neill, B.C.; Fujimori, S.; Bauer, N.; Calvin, K.; Dellink, R.; Fricko, O.; et al. The Shared Socioeconomic Pathways and their energy, land use, and greenhouse gas emissions implications: An overview. *Glob. Environ. Change* **2017**, *42*, 153–168. [CrossRef]
88. *Standard 55-2023*; Thermal Environmental Conditions for Human Occupancy. ASHRAE: Atlanta, GA, USA, 2023.
89. Zhang, Y.; Lin, K.; Zhang, Q.; Di, H. Ideal thermophysical properties for free-cooling (or heating) buildings with constant thermal physical property material. *Energy Build.* **2006**, *38*, 1164–1170. [CrossRef]
90. Salama, A. *On-Site Technical Review Report: 200 Housing Units, Wilad Djallal, Algeria*; On-Site Technical Review Report; University of Strathclyde: Glasgow, UK, 2001.
91. CNERIB. Document Technique Reglementaire Reglement Thermique du Bâtiment. In *DTR C3-T*; Centre National d'Études et de Recherches Intégrées du Bâtiment, (CNERIB), Ed.; CNERIB: Alger, Algeria, 2011.
92. Meteonorm. Available online: https://meteonorm.com/ (accessed on 18 September 2025).
93. ASHRAE. *ASHRAE Guideline 14–2014, Measurement of Energy, Demand, and Water Savings*; ASHRAE: Atlanta, GA, USA, 2014.
94. Chicco, D.; Warrens, M.J.; Jurman, G. The coefficient of determination R-squared is more informative than SMAPE, MAE, MAPE, MSE and RMSE in regression analysis evaluation. *PeerJ Comput. Sci.* **2021**, *7*, e623. [CrossRef]
95. Ruiz, G.; Bandera, C. Validation of Calibrated Energy Models: Common Errors. *Energies* **2017**, *10*, 1587. [CrossRef]
96. Ouanes, S.; Sriti, L. Regression-based sensitivity analysis and multi-objective optimisation of energy performance and thermal comfort: Building envelope design in hot arid urban context. *Build. Environ.* **2024**, *248*, 111099. [CrossRef]
97. Gossard, D.; Lartigue, B.; Thellier, F. Multi-objective optimization of a building envelope for thermal performance using genetic algorithms and artificial neural network. *Energy Build.* **2013**, *67*, 253–260. [CrossRef]